JHEP

Published for SISSA by Springer

Received: November 19, 2012
Revised: May 2, 2013
Accepted: May 10, 2013
Published: June 18, 2013

Dirac gauginos and the 125 GeV Higgs

Karim Benakli,[a] **Mark D. Goodsell**[b] **and Florian Staub**[c]

[a] *Laboratoire de Physique Theorique et Hautes Energies, CNRS, UPMC Univ Paris VI, Boite 126, 4 Place Jussieu, 75252 Paris cedex 05, France*

[b] *CPhT, Ecole Polytechnique, 91128 Palaiseau, France*

[c] *Bethe Center for Theoretical Physics & Physikalisches Institut der Universität Bonn, Nußallee 12, 53115 Bonn, Germany*

E-mail: kbenakli@lpthe.jussieu.fr, mark.goodsell@cpht.polytechnique.fr, fnstaub@th.physik.uni-bonn.de

Abstract: We investigate the mass, production and branching ratios of a 125 GeV Higgs in models with Dirac gaugino masses. We give a discussion of naturalness, and describe how deviations from the Standard Model in the key Higgs search channels can be simply obtained. We then perform parameter scans using a `SARAH` package upgrade, which produces `SPheno` code that calculates all relevant quantities, including electroweak precision and flavour constraint data, to a level of accuracy previously impossible for this class of models. We study three different variations on the minimal Dirac gaugino extension of the (N)MSSM.

Keywords: Supersymmetry Phenomenology

Open Access

doi:10.1007/JHEP06(2013)073

Contents

JHEP06(2013)073

1 Introduction

The LHC experiments have claimed the discovery of a new particle near 125 GeV [1, 2]. Its production and decays make it a good candidate for the Higgs boson. However, more experimental data is needed for a precise determination of its quantum numbers and interactions to know if the Higgs sector is the Standard Model one, or an extended version, for instance as required in supersymmetric models. A clear indication of non-minimality would be a significant excess or deficit in at least one decay channel, but the Higgs mass itself can also be regarded as such, since it is somewhat high for the most natural version of the MSSM. This is one motivation for this work, in which we study the main properties of such a Higgs boson in models with Dirac gaugino masses [3–36]. These have numerous virtues compared to their Majorana counterparts, not least that they allow for increased naturalness [6, 23, 34, 37–39] which is particularly important in the light of recent LHC SUSY searches [40–42]; but also that the direct production of gluinos is suppressed, loosening the bounds from direct LHC searches [29, 31]; they allow relaxation of flavour constraints such as due to $\mathrm{Br}(B \to s\gamma)$ [43]; they preserve R-symmetry (allowing for simpler supersymmetry-breaking models) and can be motivated from higher-dimensional theories as being derived from an $N = 2$ supersymmetry in the gauge sector at some scale.

To give gauginos Dirac masses, we must add new chiral superfields in the adjoint representation of each gauge group: a singlet $\mathbf{S} = S + \sqrt{2}\theta\chi_S + \cdots$, an SU(2) triplet $\mathbf{T} = \sum_{a=1,2,3} \mathbf{T}^{(a)} = T^{(a)} + \sqrt{2}\theta\chi_T^{(a)} + \cdots$ and an SU(3) octet $\mathbf{O} = \sum_{a=1\ldots8} O^{(a)} + \sqrt{2}\theta\chi_O^{(a)} + \cdots$. Of these, the triplet and singlet may have new renormalisable couplings with the Higgs which allow more possibilities to obtain the desired mass range than in the MSSM. More precisely, the lightest Higgs mass in these models is determined by opposite competing effects. On one hand, the presence of new couplings in the extended scalar sector leads to an enhancement of this mass by allowing new contributions to the quartic Higgs coupling. On the other hand, the supersoft operators that include the Dirac mass induce new D-term couplings, which increase Higgs mixing and thus tend to reduce the lightest Higgs mass. However, this is only potentially problematic if the triplet scalar soft mass is small; but we shall demonstrate in section 4 - along with a general discussion of naturalness in Dirac gaugino models - that it may be naturally large enough to avoid this problem. Higgs mixing involving the singlet induced by a Dirac Bino mass, however, then presents an intriguing opportunity: it allows the decays of the Higgs to b quarks and τ leptons to be suppressed while preserving the rate to Ws and Zs, and an enhancement of the diphoton rate. We give an explanation of this and a discussion of the Higgs production and decay rates in section 5.

Previous attempts to quantitatively study the Higgs sectors of Dirac gaugino models have been hampered by the lack of numerical tools to do so; until now only one-loop effective potential calculations of the Higgs mass have been possible. This is in contrast to the MSSM, where the leading corrections are known to three-loop order. However, with an upgrade of the `SARAH` package described in section 3, it is now possible to study models with arbitrary gauge groups and matter content: it can generate `SPheno` code which calculates all one-loop pole masses and tadpoles, which allows a much more accurate determination of the Higgs mass. We implement a minimal Dirac-gaugino extension of the (N)MSSM

JHEP06(2013)073

which lends itself to four particularly interesting sub-classes of models, which we review in section 2. One such class of models is the "MSSM in disguise," where all the new scalars are too heavy to observe or mix substantially with the Higgs; this is a good toy scenario to use to test of the code, and we do just that.

The `SPheno` code produced by `SARAH` can also calculate the branching ratios and production cross-sections of the Higgs, as well as electroweak precision observables such as $\Delta\rho$ and flavour constraints such as $\mathrm{Br}(B \to s\gamma)$. We take full advantage of the latter in investigating the "MSSM without μ term" [7] in section 6, comparing the results for $\Delta\rho$ with approximations given in [7]. Unfortunately those constraints in addition to those on chargino masses and the Higgs mass yield that model problematic. However, we propose a new model, which we call "dynamical μ models," in which the singlet obtains a substantial expectation value - we show in model scans in section 7 that this not only alleviates all of the problems of the MSSM without μ term, but also allows for Higgs mixing and thus interesting deviations in the Higgs production rates and branching ratios that may better fit the current data than the standard model.

2 One model into four

We shall consider the framework of e.g. [18, 23] of adding minimal fields to the MSSM to allow Dirac gaugino masses. As described above, this requires three adjoint chiral superfields $\mathbf{S}, \mathbf{T}, \mathbf{O}$ and we include the supersoft operators

$$W_{\text{supersoft}} = \int d^2\theta\sqrt{2}\theta^\alpha \Big[m_{D1}\mathbf{S}W_{Y\,\alpha} + 2m_{D2}\mathrm{tr}(\mathbf{T}W_{2\,\alpha}) + 2m_{D3}\mathrm{tr}(\mathbf{O}W_{3\,\alpha}) \Big]. \tag{2.1}$$

However, adding Dirac gaugino masses to the MSSM can introduce many extra parameters: not just the Dirac masses themselves, but also new superpotential couplings and soft terms. By making certain assumptions about the new parameters we can then arrive at different limits of the model with different phenomenology; we shall consider four such limits.

The most general renormalisable superpotential that we can write down is

$$\begin{aligned} W \;=\; & Y_u \hat{u}\hat{q}H_u - Y_d\hat{d}\hat{q}H_d - Y_e\hat{e}\hat{l}H_d + \mu\mathbf{H_u}\cdot\mathbf{H_d} \\ & + \lambda_S\mathbf{S}\mathbf{H_u}\cdot\mathbf{H_d} + 2\lambda_T\mathbf{H_d}\cdot\mathbf{T}\mathbf{H_u} \\ & + L\mathbf{S} + \frac{M_S}{2}\mathbf{S}^2 + \frac{\kappa}{3}\mathbf{S}^3 + M_T\mathrm{tr}(\mathbf{TT}) + M_O\mathrm{tr}(\mathbf{OO}) \\ & + W_2 \end{aligned} \tag{2.2}$$

where

$$W_2 = \lambda_{ST}\mathbf{S}\mathrm{tr}(\mathbf{TT}) + \lambda_{SO}\mathbf{S}\mathrm{tr}(\mathbf{OO}) + \frac{\kappa_O}{3}\mathrm{tr}(\mathbf{OOO}). \tag{2.3}$$

The usual scalar soft terms are

$$\begin{aligned} -\Delta\mathcal{L}^{\text{scalar soft}}_{\text{MSSM}} = & \left[T_u\hat{u}\hat{q}H_u - T_d\hat{d}\hat{q}H_d - T_e\hat{e}\hat{l}H_d + h.c.\right] \\ & + m^2_{H_u}|H_u|^2 + m^2_{H_d}|H_d|^2 + \left[B_\mu H_u\cdot H_d + h.c.\right] \\ & + \hat{q}^i(m^2_q)^j_i\hat{q}_j + \hat{u}^i(m^2_u)^j_i\hat{u}_j + \hat{d}^i(m^2_d)^j_i\hat{d}_j + \hat{l}^i(m^2_l)^j_i\hat{l}_j + \hat{e}^i(m^2_e)^j_i\hat{e}_j \end{aligned} \tag{2.4}$$

JHEP06(2013)073

and there are soft terms involving the adjoint scalars

$$
\begin{aligned}
-\Delta\mathcal{L}^{\text{scalar soft}}_{\text{adjoints}} &= (t_S S + h.c.) \\
&\quad + m_S^2|S|^2 + \frac{1}{2}B_S(S^2 + h.c.) + 2m_T^2\mathrm{tr}(T^\dagger T) + (B_T\mathrm{tr}(TT) + h.c.) \\
&\quad + \left[A_S\lambda_S S H_u \cdot H_d + 2A_T\lambda_T H_d \cdot T H_u + \frac{1}{3}\kappa A_\kappa S^3 + h.c.\right] \\
&\quad + 2m_O^2\mathrm{tr}(O^\dagger O) + (B_O\mathrm{tr}(OO) + h.c.)
\end{aligned} \tag{2.5}
$$

with the definition $H_u \cdot H_d = H_u^+ H_d^- - H_u^0 H_d^0$. Similarly there are the A-terms for W_2.

One limit of the above model would be to allow all parameters, including Majorana gaugino masses, to be significant and non-vanishing. Such models may have virtues due to the extra Higgs couplings and extra gaugino states (the charginos could contribute, for example, to enhancing the Higgs-to-diphoton decay channel) but we shall leave the exploration of this to future work. Instead, we shall explore models where the gaugino masses are *entirely Dirac*, taking as motivation the possibility of preserving R-symmetry in some sector of the theory (but not in all: it must ultimately be broken in any case). Of particular interest to us are:

- *MSSM in disguise*: here we shall allow a μ-term, and assume that the only source of R-symmetry violation arises in the supersymmetry-breaking sector, but permit only a B_μ term. This assumption will be preserved by renormalisation group running and so it can be justified by high-energy boundary conditions; non-zero A-terms would lead to Majorana gaugino masses. Since it is the "MSSM in disguise" we shall take the scalar singlet and triplet to be very massive (several TeV). We perform some scans over models of this type in section 3.

- *MSSM without μ term* ($\not{\mu}$SSM): this is the scenario of [7], similar to the MSSM in disguise but taking $\mu = 0$. Here we shall insist that the singlet vev is small, so the chargino mass must be generated by the coupling λ_T. We investigate this scenario in section 6.

- *Dynamical μ models*: in this scenario, we again take $\mu = 0$ but allow a substantial non-zero expectation value for the singlet. In this way, the vev and the coupling λ_S lead to an effective μ-term. Models of this type are very natural and interesting from the point of view of Higgs mixing: we perform scans over these models in section 7.

- *Dynamical μ and $B\mu$ models*: this is the scenario of [23] where we allow a non-zero κ, breaking R-symmetry in the visible sector, but allowing μ and B_μ to be generated via a non-zero singlet vev - so we can set all R-symmetry-breaking parameters in the supersymmetry breaking sector to zero. It is somewhat similar to the NMSSM, but the Dirac masses lead to some interesting differences. Models of this type can be very natural, but we leave scans of their parameter space to future work.

We review the tree-level properties of the generic case in appendix A; see also [23]. However, common to all of the above scenarios is the assumption that Dirac gaugino masses

JHEP06(2013)073

dominate over Majorana ones. For this to be natural, A-terms must also be small, so in our searches we shall set (unless otherwise stated) $W_2 = L = M_S = M_T = M_O = A_S = A_\kappa = A_T = 0$.

Some notation. We now introduce some notation relevant for the following: we redefine the singlet and triplet scalars in terms of real components $S \equiv \frac{1}{\sqrt{2}}(v_S + s_R + is_I), T^0 \equiv \frac{1}{\sqrt{2}}(v_T + T_R + iT_I)$ and have an "effective μ-term" $\tilde{\mu} \equiv \mu + \frac{1}{\sqrt{2}}(v_S\lambda_S + v_T\lambda_T)$. The expectation values v_S, v_T are associated with new non-trivial potential minimisation conditions, which we give in equation (A.7). The scalars s_R, T_R mix with the Higgs fields, with a 4×4 mass matrix given in equation (A.12); the mixing will be important in section 7.

2.1 SUSY search constraints

This paper is substantially concerned with the Higgs data from the LHC (and the Tevatron), which is summarised in appendix C, along with the relevant electroweak precision and rare decay constraints. However, the LHC (along still with LEP) has also put several limits on supersymmetric particles, which we must also take into account in model searches. Since these will be relevant for all of the following sections, we shall summarise here the relevant constraints on our models due to recent searches at the LHC. Motivated by naturalness, our models typically have several neutralinos and charginos in the hundred to a few hundred GeV mass range; these then influence the bounds on the squarks and Higgs.

2.1.1 Squarks and gluinos

In our models the gluino is a Dirac particle, and this will therefore affect the bounds on its mass - and also those of the squarks. One scenario would be to take a very heavy gluino, where the bounds on the squarks soften [29, 31]; however, in the opposite limit of a lighter gluino with heavy squarks, the bounds on the gluino mass actually strengthen. In the Majorana case, the bounds on first two generation squarks can be as high as 1.5 TeV [44] and the gluino about 1.24 TeV [45]. In the absence of an updated study for the Dirac case, we shall conservatively take the bound on first two generation squarks to be the same as in the Majorana case, and the gluino to be heavier than 1.5 TeV. However, it should be stressed that the gluino mass, coming from a supersoft operator, does not affect the other masses to the same extent as in the Majorana case.

2.1.2 Stops

Stops are now excluded up to 660 GeV for a massless neutralino [46], and indeed this bound remains roughly constant for a lightest neutralino mass up to about 200 GeV. Hence in our models, when we take the stops to be light we shall set them at 700 GeV.

2.1.3 Charginos and heavy neutralinos

The bounds on charginos and neutralinos heavier than the lightest one (the LSP) depend on whether the decays proceed via sleptons (rather than electroweak gauge bosons) and the mass of the neutralino [47]. If the sleptons are light so that the decays proceed via them, then the bounds are very strong, excluding charginos and heavy neutralinos up to

JHEP06(2013)073

600 GeV for LSP masses up to about 300 GeV (after which the bounds dramatically fall away). However, if the sleptons are much heavier than the electroweak scale (and indeed the charginos/heavy neutralinos) then the bounds are much softer - up to 315 GeV if the LSP has mass $\lesssim 110$ GeV. If the LSP is heavier than this, the bounds essentially vanish - and we are merely left with the LEP bound of 105 GeV for the chargino mass. Hence we shall simply take this to imply that the sleptons should be relatively heavy compared to the charginos and the LSP should be above about 110 GeV.

3 Numerical setup

3.1 Implementation in SARAH and SPheno

For our numerical studies we have extended the Mathematica package SARAH [48–51] to support Dirac gauginos.[1] This support includes an automatic derivation of all specific D- and fermion mass terms in the context of Dirac gauginos as well as the full two-loop RGEs using the results of ref. [39]. Both aspects are also covered in the presence of several Abelian gauge groups and kinetic mixing using the approach of ref. [52].

Afterwards we implemented our model and used the possibility of SARAH to create source code for SPheno [53, 54]. For this implementation we used the most general setup allowing all possible superpotential and soft-breaking terms of eqs. (2.2)–(2.5). Also Majorana as well as Dirac mass terms could be present at the same time. The different limits of the model were obtained by a convenient choice of the input parameters in our scans. As mentioned above, it is also possible to create a SPheno version with SARAH which includes the two-loop RGEs. In this case it is possible to study also constrained GUT models. However, we leave this for further analysis and treated nearly all parameters at the SUSY scale as independent. The only relation between parameters stems from the necessity to be at the minimum of the vacuum: since there are four non-trivial vacuum minimisation conditions (given in equations (A.5), (A.6) and (A.7)) we must use these to eliminate four parameters. From a top-down perspective, it would be preferable to specify the soft masses m_S, m_T as was done in [23], and derive from that v_S, v_T. However, the equations are non-linear in these, and so it is preferable to instead take $v_S, v_T, \tan\beta, \mu$ as input parameters in the code, and treat $m_S^2, m_T^2, m_{H_u}^2, m_{H_d}^2$ as output parameters (calculated including one-loop tadpoles). As further inputs for our studies we the soft-breaking terms as well as the superpotential couplings at the SUSY scale: the standard model gauge and Yukawa couplings are calculated at M_{SUSY} using two-loop standard model RGEs from M_Z [55].

The obtained code including these boundary conditions was compiled with SPheno 3.1.2 and provides a fully functional spectrum calculator: the entire mass spectrum is calculated at one-loop using the full dependence on the momentum of the external particle. These calculations include the entire CP and flavor structure and, of course, also the mixing between MSSM fields and the new states. For a detailed discussion of the calculation of the loop corrected mass spectrum using SARAH and SPheno for extensions of the MSSM we refer the interested reader to ref. [56]. We note that, in the absence of the theoretical

[1] The support of Dirac gauginos as well as the used model files became public with version 3.2.0 of SARAH.

JHEP06(2013)073

calculation, the code cannot include the two-loop corrections to the Higgs mass involving (Dirac) gluino masses that can be important in the MSSM and NMSSM. In those cases, the Higgs mass is usually increased by 2 to 4 GeV. Throughout we shall be conservative and allow a variation of ± 4 GeV for the mass of the Higgs in the scans, but we expect that typically the shift will be positive.

In addition, the produced `SPheno` version provides routines to calculate the decay widths and branching ratios for all SM superpartners and Higgs fields. In general, these are pure tree-level calculation. However, in the case of the Higgs particles the loop induced decays into two photons and two gluons are calculated. Here, not only the known SM or MSSM contributions are included but `SPheno` takes automatically the loops arising from all charged particles in the model into account. This calculation is comparable to the analytical results given in section 5, but also the NLO corrections due to quarks and squarks are added as given in ref. [57]. Similarly, for the Higgs decays into quarks the dominant QCD corrections due to the gluon are added [58]. Finally, the `SPheno` version for Dirac gauginos also calculates the observables $b \to s\gamma$ and $\Delta\rho$ with the same precision as done in the MSSM by `SPheno` 3.1.1 including all contributions due to the new states present in the considered model. The details of these calculations can be found in ref. [54] and references therein. With version 3.3.0 the `SPheno` output of `SARAH` provides also of a full one-loop calculation of $B^0_{s,d} \to l^+ l^-$ [59].

Of course, even if the used for this study mostly the `SPheno` output of `SARAH`, models with Dirac gauginos are supported also in all other interfaces of `SARAH`. Hence, the user can use `SARAH` to obtain model files for `CalcHep/CompHep` [60, 61], `WHIZARD/OMEGA` [62, 63], `FeynArts/FormCalc` [64, 65] or in the UFO format [66] which is supported by `MadGraph 5` [67]. The model files for `CalcHep` can also be used together with `MicrOmegas` for dark matter studies [68].

3.2 Comparison with effective potential

It is possible to calculate an approximation for the Higgs mass via the effective potential technique. In the decoupling limit of large $B\mu$, this yields

$$\begin{aligned} m_h^2 \simeq\ & M_Z^2 c_{2\beta}^2 + \frac{v^2}{2}(\lambda_S^2 + \lambda_T^2) s_{2\beta}^2 \\ & + \frac{3}{2\pi^2}\frac{m_t^4}{v^2}\left[\log\frac{m_{\tilde{t}_1} m_{\tilde{t}_2}}{m_t^2} + \frac{\mu^2 \cot^2\beta}{m_{\tilde{t}_1} m_{\tilde{t}_2}}\left(1 - \frac{\mu^2\cot^2\beta}{12 m_{\tilde{t}_1} m_{\tilde{t}_2}}\right)\right] \\ & + v^2\left[\lambda_1 c_\beta^4 + \lambda_2 s_\beta^4 + 2(\lambda_3 + \lambda_4 + \lambda_5) c_\beta^2 s_\beta^2 + 4(\lambda_6 c_\beta^2 + \lambda_7 s_\beta^2) s_\beta c_\beta\right] \\ \xrightarrow{\tan\beta\to\infty}\ & M_Z^2 + \lambda_2 v^2 + \frac{3}{2\pi^2}\frac{m_t^4}{v^2}\log\frac{m_{\tilde{t}_1} m_{\tilde{t}_2}}{m_t^2} \end{aligned} \tag{3.1}$$

where the first line is the tree-level mass, the second line is the usual contribution from stops with $m_{\tilde{t}_{1,2}}$ the physical masses and A_t set to zero; the λ_i are the coefficients of the terms in the most general CP-conserving gauge-invariant potential up to quartic order (e.g. λ_2 is the coefficient of the $|H_u|^4$ operator) about zero vev [69]. This is a good approximation when the Higgs vev is small compared to the energy scales being integrated out; in this

JHEP06(2013)073

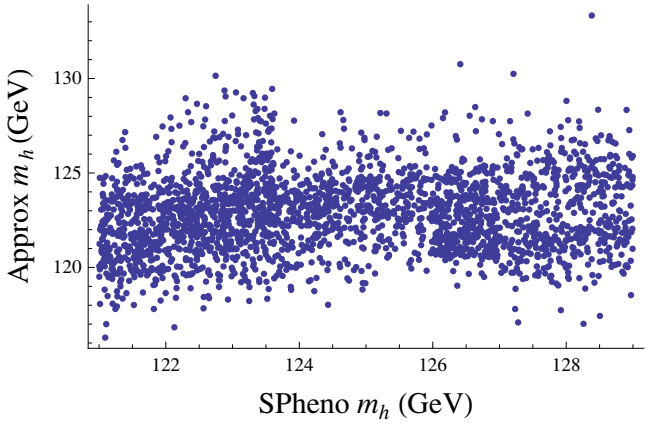

Figure 1. Comparison of effective potential method (labelled "approx m_h") with a parameter scan using `SPheno` code produced by `SARAH`. Parameters are given in the text; a searched was performed using the `SPheno` code, restricting to $m_h = 125 \pm 4\,\text{GeV}$, and from the same input parameters for each model the one-loop Higgs mass is shown (note that this has a larger range). Only models with relatively low couplings λ_S, λ_T (roughly $\lambda_S^2 + \lambda_T^2 < 1.2$).

case, we shall consider integrating out the adjoint scalars, which is appropriate for the MSSM in disguise. We give the full expression for the coefficients λ_i in appendix B, but an interesting limit is to consider $B_S = B_T = 0$ and neglect v, v_S and the Dirac masses m_{Di}; then the contribution from the singlet and triplet scalars is [23]

$$\begin{aligned} 32\pi^2\lambda_2 \supset\; & 2\lambda_S^4 \log\frac{m_S^2}{v^2} + (g_2^4 - 4g_2^2\lambda_T^2 + 10\lambda_T^4)\log\frac{m_T^2}{v^2} \\ & + \frac{4\lambda_S^2\lambda_T^2}{m_S^2 - m_T^2}\left[m_S^2 \log\frac{m_S^2}{v^2} - m_T^2\log\frac{m_T^2}{v^2} - (m_S^2 - m_T^2)\right] \\ & \overset{m_T^2\to m_S^2}{\longrightarrow} \left(g_2^4 - 4g_2^2\lambda_T^2 + 2(\lambda_S^4 - 2\lambda_S^2\lambda_T^2 + 5\lambda_T^4)\right)\log\frac{m_S^2}{v^2} \end{aligned} \tag{3.2}$$

where in the last line we show the limit that the scalar masses become equal.

By performing a scan over parameters we can compare this approximation with the more accurate results from `SPheno` using the code produced by `SARAH`; we show the results with the choice of $\tan\beta = 50$, $m_{D2} = 600\,\text{GeV}$, first two generation sfermion mass squareds of $4 \times 10^7\,(\text{GeV})^2$, third generation sfermion mass squareds $4 \times 10^6\,(\text{GeV})^2$ and scanning over $m_{D1} \in [-600, 600]\,\text{GeV}, \mu \in [-750, 750]\,\text{GeV}, B\mu \in [5000, 10^6]\,(\text{GeV})^2, \lambda_T \in [0, 1]$ while adjusting λ_S to keep $m_h = 125 \pm 4\,\text{GeV}$ in figure 1. The expectation values v_S, v_T were set by the tree level minimisation equation with $m_S^2, m_T^2 = 2.5 \times 10^7\,(\text{GeV})^2$; this resulted in values close to this for m_T^2, while the resulting one-loop adjusted values for m_S^2 varied between 10^6 and $10^{10}\,(\text{GeV})^2$. As can be seen from the figure, there is good agreement between the two, although of course the approximate effective potential calculation exhibits a wider variation of masses; that there is no apparent correlation is unsurprising, essentially reflecting the error margin in the effective potential method.

JHEP06(2013)073

4 Dirac gauginos and natural SUSY

One of the increasingly attractive features of Dirac gaugino models is that the supersoft operators allow for increased naturalness [6, 23, 34, 37–41]; they do not appear in the RGEs for the soft masses and so they only affect the stop mass via a UV-finite correction, allowing for heavy gluinos with light stops. On the other hand, the Higgs potential is corrected at tree-level by two competing effects: one is the enhancement of the Higgs mass (at low $\tan\beta$) by the new couplings λ_S, λ_T, clearly evident in equation (3.1); the other is a reduction in the effective D-term Higgs quartic coupling due to the Dirac mass terms; if we ignore the superpotential couplings and integrate out the heavy scalars then [6, 23]

$$\frac{g_Y^2+g_2^2}{8} \to \frac{1}{8}\left(\frac{m_S^2+|M_S|^2+B_S}{m_S^2+|M_S|^2+B_S+4|m_{D1}|^2}g_Y^2 + \frac{m_T^2+|M_T|^2+B_T}{m_T^2+|M_T|^2+B_T+4|m_{D2}|^2}g_2^2\right). \quad (4.1)$$

This latter effect manifests itself as mixing terms in the Higgs mass matrix (A.12) Δ_{hs}, Δ_{ht}; provided that the other soft masses are large enough the suppression can be avoided. We may then ask how large these soft masses can be while preserving naturalness, to which we consider the radiative corrections to $m^2_{H_{u,d}}$:

$$\delta m^2_{H_{u,d}} \supset -\frac{1}{16\pi^2}(2\lambda_S^2 m_S^2 + 6\lambda_T^2 m_T^2)\log\left(\frac{\Lambda}{\text{TeV}}\right) \quad (4.2)$$

where Λ is the UV cutoff of the theory. Using $\Delta \equiv \frac{\delta m_h^2}{m_h^2}$ then we have

$$\begin{aligned} m_S &\lesssim \text{TeV}\left(\frac{1}{\lambda_S}\right)\left(\frac{\log\Lambda/\text{TeV}}{3}\right)^{-1/2}\left(\frac{\Delta^{-1}}{20\%}\right)^{-1/2} \\ m_T &\lesssim 5\ \text{TeV}\left(\frac{0.1}{\lambda_T}\right)\left(\frac{\log\Lambda/\text{TeV}}{3}\right)^{-1/2}\left(\frac{\Delta^{-1}}{20\%}\right)^{-1/2}. \end{aligned} \quad (4.3)$$

The latter value is particularly important, because we also have the constraint that the triplet scalar expectation value must be small in order to avoid a large ρ parameter. We have (see appendix)

$$\Delta\rho \simeq \frac{v^2}{(m_T^2+|M_T|^2+B_T+4|m_{D2}|^2)^2}(g_2 m_{D2} c_{2\beta} + \sqrt{2}\tilde{\mu}\lambda_T)^2 \lesssim 8\times 10^{-4} \quad (4.4)$$

which is satisfied for *any* value of m_{D2} for $m_T \gtrsim 1.4$ TeV; but interestingly is also satisfied for any value of m_T if $m_{D2} \gtrsim 1.4$ TeV.

An interesting choice for the parameters λ_S, λ_T would be for them to take their $N=2$ supersymmetric values at some scale, $\lambda_S = g_Y/\sqrt{2}, \lambda_T = g_2/\sqrt{2}$, although corrections due to the running would break this exact relation. However, even if the $N=2$ scale is intermediate (such as 10^{12} GeV) assuming a desert we would still find $\lambda_S \simeq 0.2, \lambda_T \simeq 0.4$ at the low energy scale. In this case, in order to preserve naturalness we would require

$$\begin{aligned} m_S &\lesssim 2\text{TeV}\left(\frac{0.2}{\lambda_S}\right)\left(\frac{\log\Lambda/\text{TeV}}{20}\right)^{-1/2}\left(\frac{\Delta^{-1}}{20\%}\right)^{-1/2} \\ m_T &\lesssim 0.5\ \text{TeV}\left(\frac{0.4}{\lambda_T}\right)\left(\frac{\log\Lambda/\text{TeV}}{20}\right)^{-1/2}\left(\frac{\Delta^{-1}}{20\%}\right)^{-1/2}. \end{aligned} \quad (4.5)$$

JHEP06(2013)073

In order to satisfy the tree-level $\Delta\rho$ constraint, we would either need to work at small $c_{2\beta}$, or take $m_{D2} \gtrsim 1.4$ TeV and ensure that the ensuing Higgs mixing allows a large enough Higgs mass. We leave exploring this interesting possibility to future work: in this paper we shall take large values of m_T and small values of λ_T to keep the loop-level corrections to $\Delta\rho$ small.

One final naturalness-related issue in these models is that the requirement of small A-terms typically diminishes stop mixing; in the case of large $\tan\beta$ the mixing is almost eliminated. Hence the contribution from the stops to $\Delta\rho$ is [70–72]:

$$\begin{aligned}\Delta\rho^{\text{stops}} &\simeq \frac{3\alpha_{em}}{16\pi M_W^2 s_W^2} F_0(m^2_{\tilde{t}_L}, m^2_{\tilde{b}_L}) \\ &\simeq \frac{\alpha_{em}}{16\pi M_W^2 s_W^2}\frac{m_t^4}{m^2_{\tilde{t}_1}} \simeq 4\times 10^{-4}\left(\frac{500\,\text{GeV}}{m_{\tilde{t}_1}}\right)^2 \end{aligned} \tag{4.6}$$

(where $F_0(a,b) \equiv a+b-\frac{2ab}{a-b}\log\frac{a}{b}$) which is similar to the experimental value. In "natural SUSY" MSSM models, to survive the current direct search constraints the stops must be about 700 GeV (or be near the top mass), and so in the absence of large A-terms (as we are assuming) the stops by themselves will not be able to lift the Higgs mass to 125 GeV, but have a large impact on the electroweak precision corrections. On the other hand, in the context of λSUSY [72] the model can remain natural for stops as heavy as 1.5 TeV [72, 73] because the relative contribution of stops to the Higgs mass compared to the tree-level effect is small. Clearly λ_S in our models is the same as the λ in λSUSY. Hence the simplest natural scenario is to take small $\tan\beta$, small λ_T, and $\lambda_S \sim 1$ with $m_T \sim$ few TeV and $m_S \lesssim$ TeV. The Dirac gaugino masses m_{D3}, m_{D2} can be naturally large, but the Dirac Bino mass will be bounded above by the amount of mixing that it induces between the singlet and lightest Higgs (thus reducing the Higgs mass) to be a few hundred GeV. As a result of this, an amusing feature is that natural Dirac gauginos will lead to a *Majorana* neutralino, since there will be non-negligible mixing between the Bino and the neutral Higgsinos.

5 Higgs production and branching ratios

It is now important to consider the production cross-sections and branching ratios of the Higgs. In our Dirac gaugino models there is a singlet scalar which may mix with the lightest Higgs state, so we shall consider the branching ratios into each channel taking into account the mixing, providing some approximate expressions and then comparing them to the output of the `SPheno` code created by `SARAH`.

We shall use the standard definitions

$$\begin{aligned} R_i &\equiv \frac{\Gamma(h\to ii)}{\Gamma_{SM}(h\to ii)} = \left|\frac{A_{ii}}{A_{ii}^{SM}}\right|^2 \\ \mu_{ii} &\equiv \frac{\sigma(pp\to h)}{\sigma_{SM}(pp\to h)}\frac{BR(h\to ii)}{BR_{SM}(h\to ii)} \end{aligned} \tag{5.1}$$

where A_{ii} is the amplitude.

JHEP06(2013)073

To take Higgs mixing into account, consider the rotation of the states h, H, s_R via a matrix S so that

$$\begin{pmatrix} h \\ H \\ s_R \end{pmatrix} = S. \begin{pmatrix} h_1 \\ h_2 \\ h_3 \end{pmatrix}. \tag{5.2}$$

We shall assume throughout that the lightest Higgs field h_1 has mass 125 GeV, i.e. there is no additional lighter singlet. In this notation, we can then calculate how the production and decay channels are modified. At 125 GeV the production cross-sections (as listed on the CERN yellow pages [74]) are

$$\begin{aligned} \sigma_{SM}(pp \to h) = 19.5^{+14.7\%}_{-14.7\%}\text{pb} & \quad \text{gluon fusion} \\ + 1.578^{+2.8\%}_{-3\%}\text{pb} & \quad \text{vector boson fusion} \\ + 0.6966^{+3.7\%}_{-4.1\%}\text{pb} & \quad \text{WH process} \\ + 0.3943^{+5.0\%}_{-5.1\%}\text{pb} & \quad \text{ZH process} \\ + 0.1302^{+11.6\%}_{-17.1\%}\text{pb} & \quad \text{ttH process} \end{aligned}$$

Of the initial eigenstates, only h couples at tree level to the vector bosons. The coupling to gluons and in the ttH process is proportional to the top quark coupling squared, so (noting that S_{ij} are the elements of the above matrix S, so that S_{11} denotes the amount of the original state h in the physical lightest Higgs, and S_{21} is the amount of H)

$$\Gamma(gg \to h_1) \sim h_1 t\bar{t} \propto |S_{11} + S_{21} \cot\beta|^2. \tag{5.3}$$

Hence we can write

$$\begin{aligned} F_g \equiv \frac{\Gamma(gg \to h_1)}{\Gamma_{SM}(gg \to h_1)} &\simeq \frac{(19.5 + 0.1302)|S_{11} + S_{21}\cot\beta|^2 + (1.578 + 0.6966 + 0.3943)|S_{11}|^2}{22.2991} \\ &= 0.88|S_{11} + S_{21}\cot\beta|^2 + 0.12|S_{11}|^2. \end{aligned} \tag{5.4}$$

We can use the same approach for the decay branching ratios:

$$\begin{aligned} R_g, R_c \propto ht\bar{t} &\sim |S_{11} + S_{21}\cot\beta|^2 \\ R_b \propto \Gamma(h_1 \to \bar{b}b) &\sim |S_{11} - S_{21}\tan\beta|^2 \\ R_\tau \propto \Gamma(h_1 \to \bar{\tau}\tau) &\sim |S_{11} - S_{21}\tan\beta|^2 \\ R_W \propto \Gamma(h_1 \to WW^*) &\propto |S_{11}|^2 \\ R_Z \propto \Gamma(h_1 \to ZZ^*) &\propto |S_{11}|^2. \end{aligned} \tag{5.5}$$

Since the photon couples at one loop to the Higgs, and the singlet couples to charged fields, the expression for the coupling to the photon will be more complicated. At $m_h = 125$ GeV, the standard model Higgs branching ratio (as listed on the CERN yellow pages [74]) is dominated by

$$\begin{aligned} BR_{SM}(h_1 \to \bar{b}b) &= 5.77 \times 10^{-1} \\ BR_{SM}(h_1 \to WW^*) &= 2.15 \times 10^{-1} \end{aligned}$$

JHEP06(2013)073

$$
\begin{aligned}
BR_{SM}(h_1 \to gg) &= 8.6 \times 10^{-2} \\
BR_{SM}(h_1 \to \tau\tau) &= 6.3 \times 10^{-2} \\
BR_{SM}(h_1 \to \bar{c}c) &= 2.91 \times 10^{-2} \\
BR_{SM}(h_1 \to ZZ^*) &= 2.6 \times 10^{-2}
\end{aligned} \tag{5.6}
$$

So we can write

$$
\begin{aligned}
\mu_{XX} &= F_g \frac{R_X(1 - \mathrm{Br}(h \to \text{invisible}))}{\sum_Y R_Y \mathrm{Br}_{SM}(h \to Y)} \\
&\simeq F_g \frac{R_X(1 - \mathrm{Br}(h \to \text{invisible}))}{0.640|S_{11} - S_{21}\tan\beta|^2 + 0.241|S_{11}|^2 + 0.115|S_{11} + S_{21}\cot\beta|^2}.
\end{aligned} \tag{5.7}
$$

To approximate the diphoton channel, we require the expression

$$
R_\gamma = \left| \frac{1}{A_{\gamma\gamma}^{SM}} \frac{v}{2} \left[\frac{g_{h_1 VV}}{m_V^2} Q_V^2 A_1(\tau_V) + \frac{2 g_{h_1 ff} N_C Q_f^2}{m_f} A_{1/2}(\tau_f) + \frac{g_{h_1 SS} N_C Q_S^2}{m_S^2} A_0(\tau_S) \right] \right|^2 \tag{5.8}
$$

where the functions A_s where s is the spin of the field in the loop are standard and given in [57]; $\tau_X \equiv 4m_X^2/m_{h_1}^2$. For fermions and scalars they are well approximated by the large mass limits of 4/3 and 1/3 respectively, but for the W boson and top quark the values are $A_1(\tau_W) \simeq -8.32, (4/3)A_{1/2}(\tau_t) \simeq 1.84$. If we consider that the singlet couples to some charged Dirac fermion we can write for the couplings $g_{h_1 ii}$

$$
\begin{aligned}
g_{h_1 VV} &= \frac{2M_V^2}{v} S_{11} \\
g_{h_1 t\bar{t}} &= \frac{m_t}{v}(S_{11} + \cot\beta S_{21}) \\
g_{h_1 b\bar{b}} &= \frac{m_b}{v}(S_{11} - \tan\beta S_{21})
\end{aligned} \tag{5.9}
$$

We can then consider enhancements through various fields remaining light, taking the mixing into account.

5.1 Charginos

The chargino mass matrix is expanded by new charged states from the triplet: in the basis $(T^+, \tilde{W}^+, H_u^+)/(T^-, \tilde{W}^-, H_d^+)$ it is

$$
M_{Ch} = \begin{pmatrix} M_T + \frac{v_S \lambda_{ST}}{\sqrt{2}} & m_{2D} + g_2 v_T & \lambda_T v c_\beta \\ m_{2D} - g_2 v_T & M_2 & g_2 v s_\beta/\sqrt{2} \\ -\lambda_T v s_\beta & g_2 v c_\beta/\sqrt{2} & \tilde{\mu} - \sqrt{2}\lambda_T v_T \end{pmatrix} \tag{5.10}
$$

With $v_T \simeq 0$ and defining $\tilde{M}_T \equiv M_T + \frac{v_S \lambda_{ST}}{\sqrt{2}}$ this has determinant

$$
\det(M_{Ch}) = \frac{1}{4}\left[-4(m_{2D}^2 - M_2 \tilde{M}_T)\tilde{\mu} + 2\sqrt{2} g_2 \lambda_T m_{2D} v^2 c_{2\beta} + (\lambda_T^2 M_2 - 2g_2^2 \tilde{M}_T) v^2 s_{2\beta} \right]. \tag{5.11}
$$

JHEP06(2013)073

Since the loop function $A_{1/2}$ varies very little between the lower bound on chargino masses from LEP (105 GeV, or 92 GeV with caviats) and infinite mass, it is very well approximated by 4/3 over all cases of interest. Then we can well approximate

$$\begin{aligned} A_{\gamma\gamma}^{\text{Charginos}} &= \sum_f S_{11}\frac{vg_{hff}}{m_f}A_{1/2}(\tau_f) + S_{21}\frac{vg_{Hff}}{m_f}A_{1/2}(\tau_f) + S_{31}\frac{vg_{s_Rff}}{m_f}A_{1/2}(\tau_f) \\ &\simeq \frac{4}{3}v\left[S_{11}\partial_h \log\det m_f + S_{21}\partial_H \log\det m_f + S_{31}\partial_{s_R}\log\det m_f\right] \\ &\simeq \frac{4}{3}\frac{v}{\det M_{Ch}}\left[\frac{v}{2}S_{11}\left(2\sqrt{2}g_2\lambda_T m_{D2}c_{2\beta} + (2M_2\lambda_T^2 - g_2^2\tilde{M}_T^2)s_{2\beta}\right)\right. \\ &\qquad - \frac{v}{2}S_{21}\left(2\sqrt{2}g_2\lambda_T m_{D2}s_{2\beta} - (2M_2\lambda_T^2 - g_2^2\tilde{M}_T^2)s_{2\beta}\right) \\ &\qquad \left. - \frac{1}{\sqrt{2}}S_{31}\left(\lambda_S(m_{D2}^2 - M_2\tilde{M}_T) + \lambda_{ST}\left(\frac{1}{4}g_2^2v^2s_{2\beta} - M_2\tilde{\mu}\right)\right)\right] \end{aligned} \tag{5.12}$$

In the limit $M_2 = M_T = \lambda_{ST} = 0$, this simplifies to

$$A_{\gamma\gamma}^{\text{Charginos}} \simeq \frac{4}{3}\frac{1}{\sqrt{2}m_{D2}\tilde{\mu} - g_2v^2\lambda_T c_{2\beta}}\left[2g_2\lambda_T v^2(-c_{2\beta}S_{11} + s_{2\beta}S_{21}) + \lambda_S v m_{D2}S_{31}\right]. \tag{5.13}$$

The scenario of light charginos is particularly appropriate for the MSSM in disguise; since the adjoint scalars are all massive the main phenomenological difference with the MSSM will be the charginos and neutralinos. Hence this represents one useful limit of this formula, where there is negligible mixing between the Higgs states (i.e. $S_{11} \simeq 1, S_{i1} \simeq 0\ \forall\ i \neq 1$). Then it is clear that for an appreciably large coupling λ_T and large $c_{2\beta}$ the $\gamma\gamma$ channel can be enhanced *without affecting the other channels*. We performed at scan at $\lambda_T = 1, \tan\beta = 50$ varying μ, and plot the contours of the Higgs to diphoton branching ratio in figure 2, showing also the effect on $\Delta\rho$. This analysis is similar in spirit to models adding a triplet to the MSSM [75], except instead of including a Majorana Wino and supersymmetric triplet mass we have included a Dirac Wino mass.

An alternative application of formula (5.13) is to allow appreciable Higgs mixing but take the large m_{D2} limit, leaving light Higgsinos. We then find

$$R_\gamma \simeq \left|S_{11} - 0.28\cot\beta S_{21} - 0.15\frac{v\lambda_S}{\mu}S_{31}\right|^2. \tag{5.14}$$

Hence the diphoton production rate can be enhanced for suitably large $v\lambda_S/\mu$ and S_{31}. This is applicable for the NMSSM too, and is particularly interesting because by varying the Higgs mixing terms we can simultaneously enhance $\mu_{\gamma\gamma}$, decrease the $\mu_{b\bar{b}}$ and $\mu_{\tau\bar{\tau}}$ while maintaining μ_{WW} and μ_{ZZ} roughly unchanged if so desired. This is similar to singlet extensions of the MSSM without Dirac gauginos [76] and can be easily understood from equations (5.5) and (5.7): by having a small positive admixture of H we enhance the coupling of the Higgs to tops, and hence to gluons; by reducing S_{11} we reduce the coupling to bottoms and taus, which reduces the total width of the Higgs - both of these can compensate for the reduction in coupling to Ws. In figure 3 we show how μ_{bb} and $\mu_{\tau\tau}$ are affected by the mixing. The above effect of the mixing and charginos on $\mu_{\gamma\gamma}$ is then illustrated in figures 4 and 5.

JHEP06(2013)073

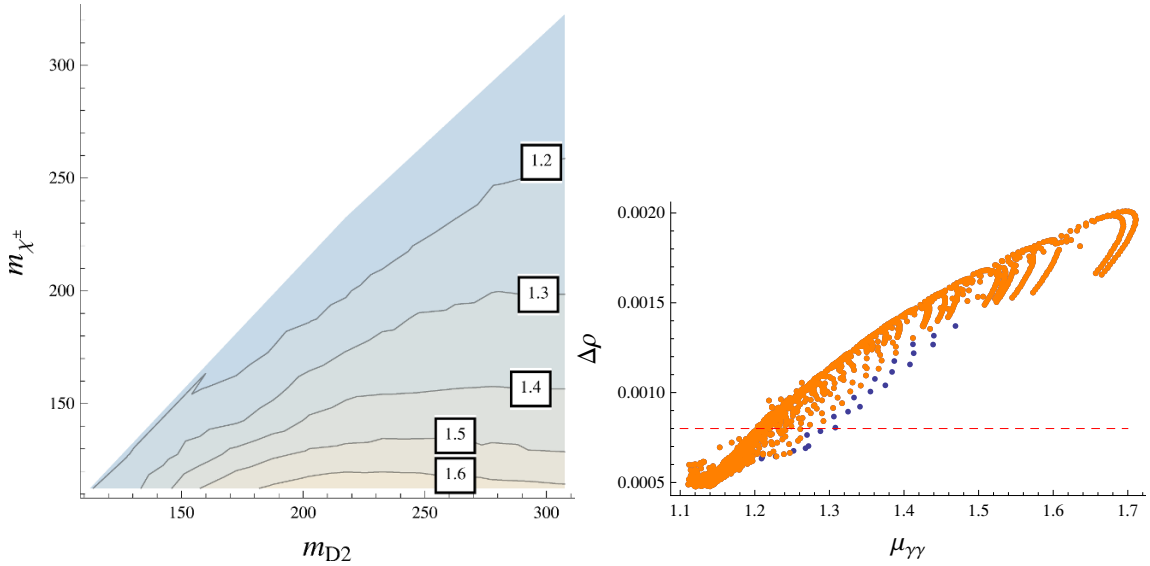

Figure 2. Results of a scan over a subspace of the "MSSM in disguise" with $\lambda_T = 0.7$, $\tan\beta = 50$, varying m_{D2} and μ in order to vary the lightest chargino mass which is restricted to be Dirac Wino-like (above the contour the lightest chargino is Higgsino-like). The stop and sbottom masses were taken to be equal and varied in order to keep the Higgs mass at 125 ± 4 GeV (within reasonable accuracy of the results of the `SARAH`-produced `SPheno` code, which cannot include two-loop effects due to the Dirac gluino). Other non-zero soft parameters were: $m_{D1} = 200$ GeV, $m_{D3} = 1000$ GeV, $\lambda_S = 0.1$ (the gluino mass is technically just too low for current limits, but we have verified that raising the gluino mass above current bounds does not noticeably affect the result); the slepton and first two generations of squark masses squared were 4×10^7 (GeV)^2; the singlet and triplet scalar masses were approximately 5000 GeV; $B\mu$ was varied over $[300, 5 \times 10^5]$ (GeV)^2. Left: contours of $\mu_{\gamma\gamma}$ (GeV). Right: $\mu_{\gamma\gamma}$ vs $\Delta\rho$; orange points have the lightest chargino mass greater than 105 GeV, blue ones smaller. The value 0.0008, usually taken as a (2σ) upper bound, is shown as the red dashed line.

5.2 Charged Higgs

The charged Higgs fields can also contribute to the diphoton rate in these models. The full charged Higgs matrix involves not just the $H^\pm$ of the MSSM, but also the charged triplet scalars; however, from the ρ-parameter constraint we know that the triplet scalars must be heavy (see section 4), so we shall neglect their contribution. Hence we can approximate

$$A_{\gamma\gamma}^{\text{Charged Higgs}} \simeq \frac{v^2}{3m_{H^\pm}^2}\frac{1}{16}\Bigg[-S_{11}\left(g_Y^2 - 3g_2^2 + 2\lambda_S^2 - 14\lambda_T^2 + (g_Y^2 + g_2^2 - 2(\lambda_S^2 + \lambda_T^2))\cos 4\beta\right) + S_{21}(g_Y^2 + g_2^2 - 2(\lambda_S^2 + \lambda_T^2))\sin 4\beta + \frac{8S_{31}}{v}\left(g_Y m_{D1} c_{2\beta} + \sqrt{2}\lambda_S(\tilde{\mu} + \frac{1}{\sqrt{2}}\kappa v_S s_{2\beta} + \frac{1}{2}A_S s_{2\beta}\right)\Bigg] \quad (5.15)$$

A large contribution to the diphoton rate from charged Higgs loops can then arise when mixing between the lightest Higgs and the singlet is substantial. Note that light charged Higgs fields in the limit of very small $\tan\beta$ also often demand light stops and charginos to cancel large contributions to $b \to s\gamma$.

JHEP06(2013)073

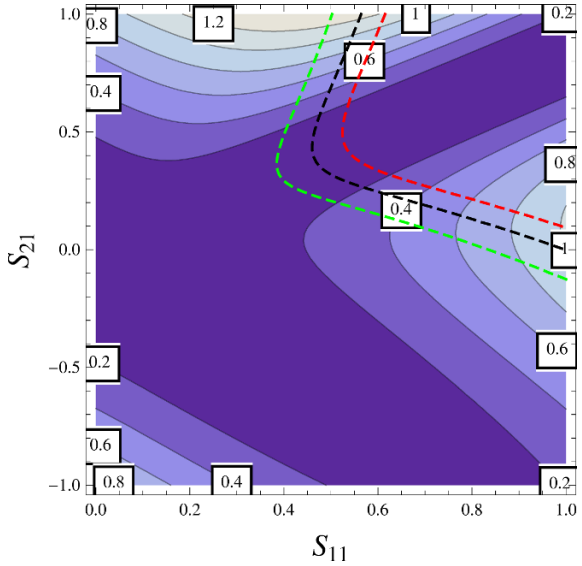

Figure 3. Contours of μ_{bb} or equivalently $\mu_{\tau\tau}$ with $\tan\beta = 1.2$, given as functions of the elements of the neutral Higgs mixing matrix S (so that S_{11} denotes the amount of the original state h in the physical lightest Higgs, and S_{21} is the amount of H). The dashed lines represent $\mu_{WW} = 1.3$ (red), 1 (black) and 0.7 (green).

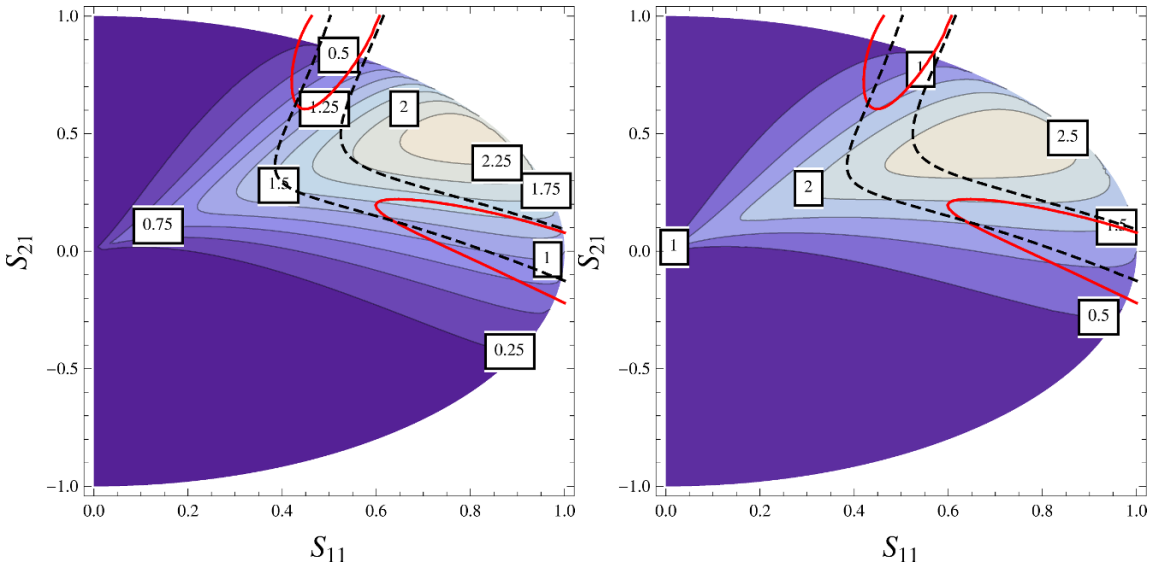

Figure 4. Contours of $\mu_{\gamma\gamma}$ for $\lambda_S v/m_{\chi^+} = -2$ (left) and -3 (right) with $\tan\beta = 1.2$ as functions of the Higgs mixing matrix S. The black dashed lines are contours of $\mu_{WW} = 1.0 \pm 0.3$, and the red contour is a rough 95% confidence-level preferred region according to the data given in appendix C (excluding electroweak precision data, which is dependent on the spectra of any other light particles).

5.3 Stops and staus

Of the squarks in the theory, the stops and staus - having the strongest couplings to the light Higgs - have been studied in the MSSM as candidates to modify the Higgs to dipho-

JHEP06(2013)073

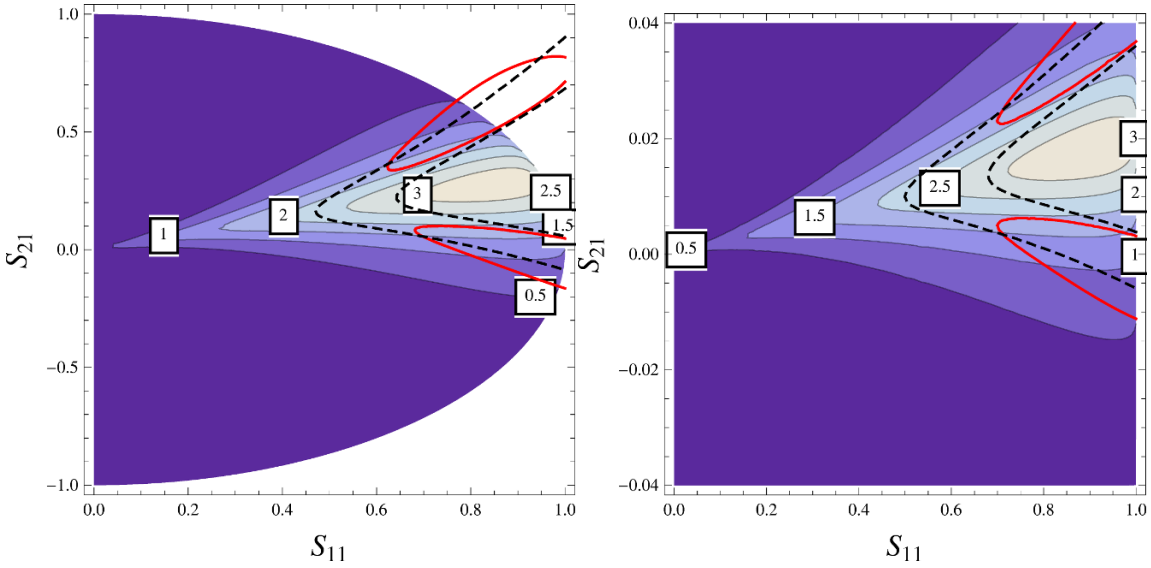

Figure 5. Contours of $\mu_{\gamma\gamma}$ for $\lambda_S v/m_{\chi^+} = -3$, $\tan\beta = 3$ (left) and 50 (right) as functions of the Higgs mixing matrix S. The black dashed lines are contours of $\mu_{WW} = 1.0 \pm 0.3$, and the red contour is a rough 95% confidence-level preferred region according to the data given in appendix C (excluding electroweak precision data, which is dependent on the spectra of any other light particles).

ton rate [77, 78]. In models with Dirac gauginos, the new D-term contributions to the potential modify the squark masses; for the stop and stau their mass matrices are given in appendix equations (A.19) and (A.20). Neglecting the normal D-term components, v_T and the A-terms gives approximately

$$\mathcal{M}_{\tilde{t}}^2 \simeq \begin{pmatrix} m_Q^2 + \frac{1}{3} g_Y m_{D1} v_S + v^2 \frac{1}{2} y_t^2 s_\beta^2 & -\frac{1}{\sqrt{2}} v y_t \tilde{\mu} c_\beta \\ -\frac{1}{\sqrt{2}} v y_t \tilde{\mu} c_\beta & m_{t_R}^2 - \frac{4}{3} g_Y m_{D1} v_S + v^2 \frac{1}{2} y_t^2 s_\beta^2 \end{pmatrix}$$
$$\mathcal{M}_{\tilde{\tau}}^2 = \begin{pmatrix} m_L^2 - g_Y m_{D1} v_S + v^2 \frac{1}{2} y_\tau^2 c_\beta^2 & -\frac{1}{\sqrt{2}} v y_\tau \tilde{\mu} s_\beta \\ -\frac{1}{\sqrt{2}} v y_\tau \tilde{\mu} s_\beta & m_{\tau_R}^2 + 2 g_Y m_{D1} v_S + v^2 \frac{1}{2} y_t^2 c_\beta^2 \end{pmatrix}. \tag{5.16}$$

It is straightforward to derive expressions for the the couplings of the stops and staus to the Higgs eigenstates, but since the full expressions are lengthy we give here simplified formulae neglecting subleading terms proportional to M_Z and setting the A-terms and v_T to zero:

$$A_{\gamma\gamma}^{\text{Stops}} \simeq \frac{4 m_t^2}{9 m_{\tilde{t}_1}^2 m_{\tilde{t}_2}^2} \Big[S_{11} \Big(m_{\tilde{t}_1}^2 + m_{\tilde{t}_2}^2 - \tilde{\mu}^2 \cot^2\beta \Big) + S_{21} \Big(m_{\tilde{t}_1}^2 + m_{\tilde{t}_2}^2 + \tilde{\mu}^2 \Big) \cot\beta \tag{5.17}$$
$$- S_{31} \Big(\frac{1}{\sqrt{2}} v \lambda_S \tilde{\mu} \cot^2\beta + \frac{m_{D1} M_Z s_W}{3 m_t^2} \Big(3 m_t^2 + 4 m_Q^2 - m_U^2 \Big) \Big) \Big]$$
$$A_{\gamma\gamma}^{\text{Staus}} \simeq \frac{m_\tau^2}{3 m_{\tilde{\tau}_1}^2 m_{\tilde{\tau}_2}^2} \Big[S_{11} \Big(m_{\tilde{\tau}_1}^2 + m_{\tilde{\tau}_2}^2 - \tilde{\mu}^2 \tan^2\beta \Big) - S_{21} \Big(m_{\tilde{\tau}_1}^2 + m_{\tilde{\tau}_2}^2 + \tilde{\mu}^2 \Big) \tan\beta \tag{5.18}$$
$$- S_{31} \Big(\frac{1}{\sqrt{2}} v \lambda_S \tilde{\mu} \tan^2\beta - \frac{m_{D1} M_Z s_W}{m_\tau^2} \Big(2 m_L^2 - m_E^2 + m_\tau^2 \Big) \Big) \Big].$$

JHEP06(2013)073

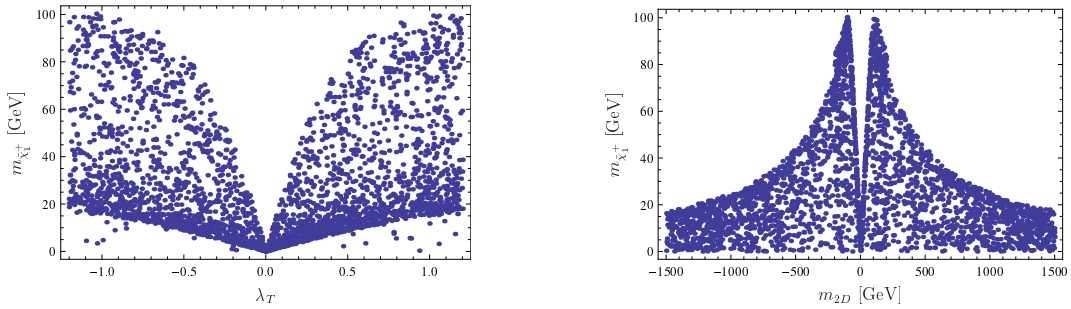

Figure 6. Mass of the lightest charginos as function of λ_T (left) and m_{2D} (right). The others parameters have been chosen in the ranges: $\tan\beta = [30, 70]$, $\lambda_S = [-0.2, 0.2]$, $\lambda_{ST} = \kappa = [-1.7, 1.7]$, $B_S = B_T = [-10^7, 10^7]$ GeV, $B_\mu = [-100, 100]$ GeV, $v_T = v_S = [-1, 1]$ GeV, $m_{1D} = [-1.5, 1.5]$ TeV, $T_{\rm top} = [-1.5, 1.5]$ TeV. The sfermion sector is fixed by $m^2_{q,ii} = m^2_{d,ii} = m^2_{u,ii} = 5 \cdot 10^6$ GeV^2, $m^2_{e,ii} = m^2_{l,ii} = 5 \cdot 10^5$ GeV^2 $(i = 1, 2)$, $m^2_{q,33} = m^2_{d,33} = m^2_{u,33} = 10^6$ GeV^2, $m^2_{e,33} = m^2_{l,33} = 10^5$ GeV^2.

Here $m_{\tilde{t}_i}, m_{\tilde{\tau}_i}$ are the masses of the stop and stau eigenstates respectively. The Dirac mass enters into the above by shifting the mases (e.g. $m^2_{\tilde{t}_1} + m^2_{\tilde{t}_2} = m^2_Q + m^2_U + 2m^2_t - g_Y m_{D1} v_S$) but clearly only plays a significant role in enhancing the diphoton channel if there is large mixing of the lightest Higgs with the singlet scalar.

6 MSSM without μ-term

In the presence of Dirac gaugino masses it is possible to remove the Higgsinos' mass term from the superpotential of the MSSM [7]. This is another way of curing the intrinsic μ-problem of the MSSM. Furthermore, an approximate $\mathrm{U}(1)_R$ symmetry naturally guarantees that $\tan\beta$ is large, explaining the top/bottom quark mass hierarchy. In contrast to its appealing theoretical aspact, the $\not{\mu}$SSM is under substantial pressure from experimental data. First, LEP put a lower limit on the mass of the lightest chargino of 94 GeV [79]. The chargino mass eq. (5.10) reads in this limit

$$M_{Ch} = \begin{pmatrix} 0 & m_{2D} & \lambda_T v c_\beta \\ m_{2D} & 0 & g_2 v s_\beta/\sqrt{2} \\ -\lambda_T v s_\beta & g_2 v c_\beta/\sqrt{2} & 0 \end{pmatrix} \tag{6.1}$$

It is known that it is possible to fulfill this bound by a careful choice of λ_T and m_{2D}: a large value of λ_T as well as m_{2D} around 107 GeV is needed to maximize the mass of the lightest chargino, see figure 6. The highest mass which can be reached at tree-level is about 110 GeV. This is also not improved at the one-loop level because the loop corrections due to the heavy triplets even tend to decrease the mass. Hence, the highest mass we could find in our scans calculating the full one-loop spectrum was 103 GeV. This is already under heavy pressure using the latest results for electroweakino searches at LHC and LEP, see section 2.1.3. Hence, one would need special mass configurations like compressed spectra in order to soften the mass limit and somehow keep this model alive.

JHEP06(2013)073

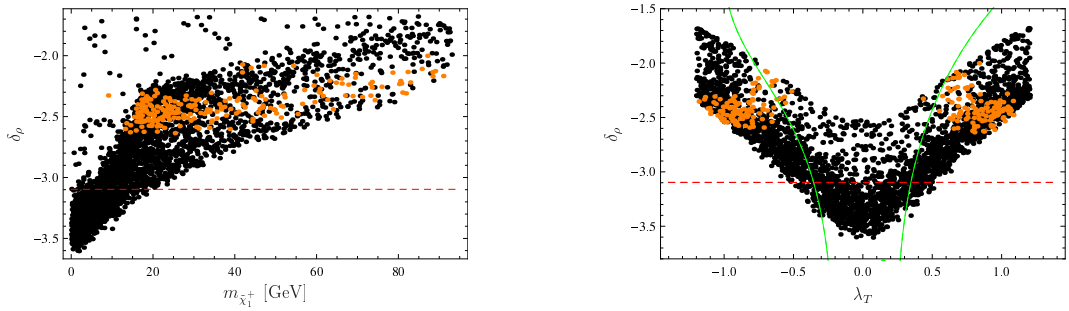

Figure 7. Left: $\delta_\rho \equiv \log_{10} \Delta\rho$ versus the lightest chargino mass. The orange points indicate a mass of the lightest Higgs in the range of 122–128 GeV. The dashed, red line indicates $\delta\rho < 8 \cdot 10^{-4}$. Right: δ_ρ as function of λ_T. The green line shows the result using the approximative formula given in ref. [7]. The input values are the same as for figure 6.

However, a more severe problem is that the large values of λ_T lead often to a huge contribution to $\Delta\rho$. The reason is that this coupling breaks the custodial $SU(2)_L$ symmetry present in the SM and MSSM: especially, the chargino and neutralino-loops contribute differently to the W and Z self-energies. The large impact was already pointed out in ref. [7] using an approximation for the resulting contributions to the T-parameter. We repeat this analysis with the full numerical evaluation of $\Delta\rho$. We find a strong correlation in this model between the mass of the lightest chargino and the smallest possible value of $\Delta\rho$ as depicted in figure 7.

Even if the full calculations leads to somewhat smaller values of $\Delta\rho$ than the approximate one for $\lambda_T > 1$, all points which fulfill the limit of $m_{\tilde{\chi}_1^+} > 94\,\text{GeV}$ suffer from a large $\Delta\rho$ of at least 0.003. Many points are even above 0.01. Note that $\Delta\rho$ is very quickly increasing with the chargino mass. Therefore, demanding $\Delta\rho < 0.0008$ would rule out all points with chargino masses above 20 GeV. Furthermore, it can also be seen that in general the points with a Higgs mass between 122 and 128 GeV lead independently from the chargino mass to $\Delta\rho > 0.001$. The reason is that a sizable contribution of λ_T to the tree-level Higgs mass is needed. This could, of course, be circumvented to some extent by allowing for even larger values of T_{top}. However, this is in contradiction to the approximate $U(1)_R$-symmetry which suppresses in general the trilinear terms. Therefore, if we restrict ourself to moderate values of the squared squark mass parameters and trilinear soft-term, this model is always in conflict with $\Delta\rho$: even if it would be somehow possible to find kinematical configurations to significantly reduce the LEP limits on the chargino mass, the now existing bound on the Higgs mass still predicts too large values of $\Delta\rho$.

7 Dynamical μ models

Although the "MSSM without μ term" may be severely challenged, by allowing a substantial expectation value for the singlet the various problems can be cured. The Higgs potential will always lead to a non-zero value for v_S as can be seen from the minimisation condition (A.16), but in order for this to be significant we can allow a non-zero negative

JHEP06(2013)073

value for B_S and/or a non-zero tadpole term t_S. Both of these are generically present and do not break R-symmetry. In this scenario, as in the MSSM without μ term, we take the only significant source of R-symmetry breaking to be a $B\mu$ term.

This scenario is particularly interesting from the perspective of Higgs mixing, since the singlet adjoint scalar will typically be light - we see from the minimisation conditions that the parameter $\tilde{m}_S^2$ in the tree-level mass-squared matrix (A.12) is

$$\tilde{m}_S^2 = -\frac{\sqrt{2}t_S + v_0^3}{v_S} \tag{7.1}$$

and, expecting from naturalness and RGE running [39] $t_S \sim v_0^3 \sim v^3, v_S \sim v$, $\tilde{m}_S^2 \sim v^2$. There may thus be substantial mixing between the singlet and original "h" eigenstate; the size of $B\mu$ term then controls the amount of "H" in the lightest Higgs mass eigenstate.

Moreover, the singlet couples to the gauginos via the coupling λ_S, which, if m_{D2} is not small, will be predominantly Higgsino-like. This then offers the possibility of realising the scenario considered in section 5.1. We have therefore conducted a scan over a portion of the parameter space of these models, concentrating on models with a small component of mixing between h and H but substantial S_{11} and S_{31} components, using the `SPheno` code produced by `SARAH`. $\tan\beta$ was taken to be 1.5 and λ_S was varied from a negative initial value in order to fix the Higgs mass at $125 \pm 4\,\text{GeV}$ - recall that this is a rather conservative error range. The other parameters varied were $m_{D1} \in [-800, 800]\,\text{GeV}, v_S \in [130, 430]\,\text{GeV}, B\mu \in [312, 90312]\,(\text{GeV})^2$, while the non-zero fixed soft parameters were $\lambda_T = 0.021, B_S = -5 \times 10^5\,(\text{GeV})^2, t_S = -1.5 \times 10^7\,\text{GeV}^3, m_T^2 = 2.5 \times 10^7\,(\text{GeV})^2, m_O^2 = 9 \times 10^6\,(\text{GeV})^2, m_{D2} = 600\,\text{GeV}, m_{D3} = 1500\,\text{GeV}$. The slepton and first two generations of squark masses squared were $4 \times 10^7\,(\text{GeV})^2$ while the third generation squark masses squared were $1.5 \times 10^6\,(\text{GeV})^2$.

Figure 8 shows the μ_{WW} and $\mu_{\tau\tau}$ values versus $\mu_{\gamma\gamma}$ (μ_{ZZ} and μ_{bb} being, as per the approximate formulae, almost identical to μ_{WW} and $\mu_{\tau\tau}$ respectively) while also giving the values of $\Delta\rho$ and $\text{BR}(b \to s\gamma)$. As can be seen from the plots, there are many experimentally viable model points. To further elucidate the comparison with our predicted scenario, a plot of the mixing parameters S_{11} and S_{21} with $\mu_{\gamma\gamma}$ revealed by the colour of the points is shown in figure 9.

It is worthwhile to pick out one example point; this has $\lambda_S = -1.5, B\mu = 7.57 \times 10^4\,(\text{GeV})^2, v_S = 161\,\text{GeV}$, $m_{D1} = -391\,\text{GeV}$ which leads to light neutral Higgs masses (at one loop) of $122, 300, 428\,\text{GeV}$, a light pseudoscalar Higgs mass of $382\,\text{GeV}$, neutralinos of mass $130, 173, 428, 474, 649, 652\,\text{GeV}$ and charginos of masses $165, 648, 653\,\text{GeV}$. The mixing data is which results in $S_{11} = 0.91, S_{21} = 0.1, S_{31} = -0.4$ which results in $\mu_{\gamma\gamma} = 1.77, \mu_{WW} = 1.24, \mu_{ZZ} = 1.07, \mu_{bb} = 0.83, \mu_{\tau\tau} = 0.89$ and $\Delta\rho = 1.6 \times 10^{-4}, \text{BR}(b \to s\gamma) = 3.4 \times 10^{-4}$.

Models with light stops. In the previous scan, we held the third generation masses to be heavy to be above search bounds and to diminish their contribution to $\Delta\rho$ whilst still remaining natural. However, it is also straightforward to find models of the above class that have light stops, which would be natural even for the MSSM but also interesting for

JHEP06(2013)073

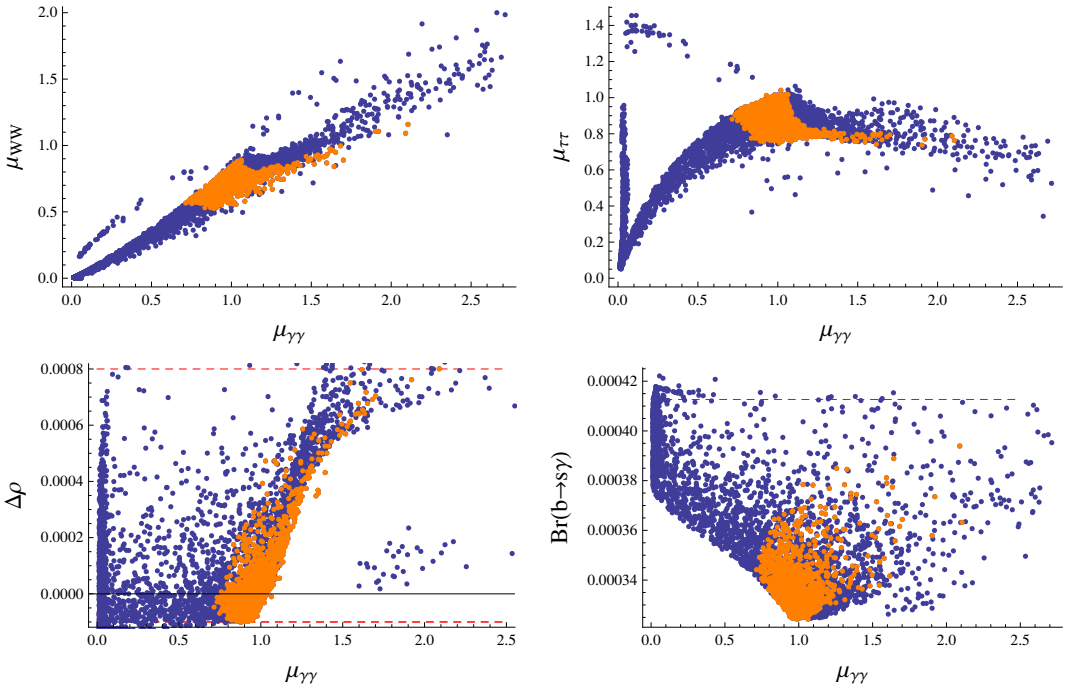

Figure 8. Production cross-section times branching ratio for a scan of a subspace of the "dynamical μ" scenario, with parameters chosen to enhance Higgs mixing. In the scan, $\tan\beta$ was taken to be 1.5 and λ_S was varied in order to fix the Higgs mass at $125 \pm 4\,\text{GeV}$ with inital value being negative. The other parameters varied were $m_{D1} \in [-800, 800]\,\text{GeV}, v_S \in [130, 430]\,\text{GeV}, B\mu \in [312, 90312]\,(\text{GeV})^2$, while the non-zero fixed soft parameters were $\lambda_T = 0.021, B_S = -5 \times 10^5\,(\text{GeV})^2, t_S = -1.5 \times 10^7\,\text{GeV}^3, m_T^2 = 2.5 \times 10^7\,(\text{GeV})^2, m_Q^2 = 9 \times 10^6\,(\text{GeV})^2, m_{D2} = 600\,\text{GeV}, m_{D3} = 1500\,\text{GeV}$. The slepton and first two generations of squark masses squared were $4 \times 10^7\,(\text{GeV})^2$ while the third generation squark masses squared were $1.5 \times 10^6\,(\text{GeV})^2$. The points shown in orange pass all experimental limits and furthermore lie within a crude 95% confidence limit via χ^2 based on the current Higgs and electroweak precision data as described in appendix C.

LHC searches. Taking the same fixed values as above except now with third generation soft masses at $(700\,\text{GeV})^2, m_{D2} = 1\text{TeV}, \tan\beta = 2$, one example has $\lambda_S = -0.96, B\mu = 3.5 \times 10^4\,(\text{GeV})^2, v_S = 193\,\text{GeV}$ and $m_{D1} = -294\,\text{GeV}$ which leads to $v_T = 0.46\,\text{GeV}$, light neutral Higgs masses of $124, 257, 360\,\text{GeV}$, a light pseudoscalar Higgs mass of 290, a light charged Higgs mass of 255 GeV, neutralinos of masses $116, 140, 320, 344\,\text{GeV}$ and charginos of masses $130, 1059, 1062\,\text{GeV}$. The mixing data is $S_{11} = 0.97, S_{21} = 0.03, S_{31} = -0.24$ which results in $\mu_{\gamma\gamma} = 1.3, \mu_{WW} = 1.1, \mu_{ZZ} = 0.98, \mu_{bb} = 0.97, \mu_{\tau\tau} = 1.02$ and $\Delta\rho = 3.4 \times 10^{-4}, \text{BR}(b \to s\gamma) = 3.46 \times 10^{-4}$.

Another example with more mixing has $\lambda_S = -1.14, B\mu = 4.6 \times 10^4\,(\text{GeV})^2, v_S = 178\,\text{GeV}$ and $m_{D1} = -283\,\text{GeV}$ which leads to $v_T = 0.47\,\text{GeV}$, light neutral Higgs masses of $122, 288, 380\,\text{GeV}$, a light pseudoscalar Higgs mass of 328, a light charged Higgs mass of 281 GeV, light neutralinos of masses $115, 152, 319, 355\,\text{GeV}$ and charginos of masses 141 GeV and a TeV. The mixing data is $S_{11} = 0.95, S_{21} = 0.06, S_{31} = -0.31$ which results in $\mu_{\gamma\gamma} = 1.5, \mu_{WW} = 1.2, \mu_{ZZ} = 1.0, \mu_{bb} = 0.91, \mu_{\tau\tau} = 0.96$ and $\Delta\rho = 6 \times 10^{-4}, \text{BR}(b \to s\gamma) = 3.4 \times 10^{-4}$.

JHEP06(2013)073

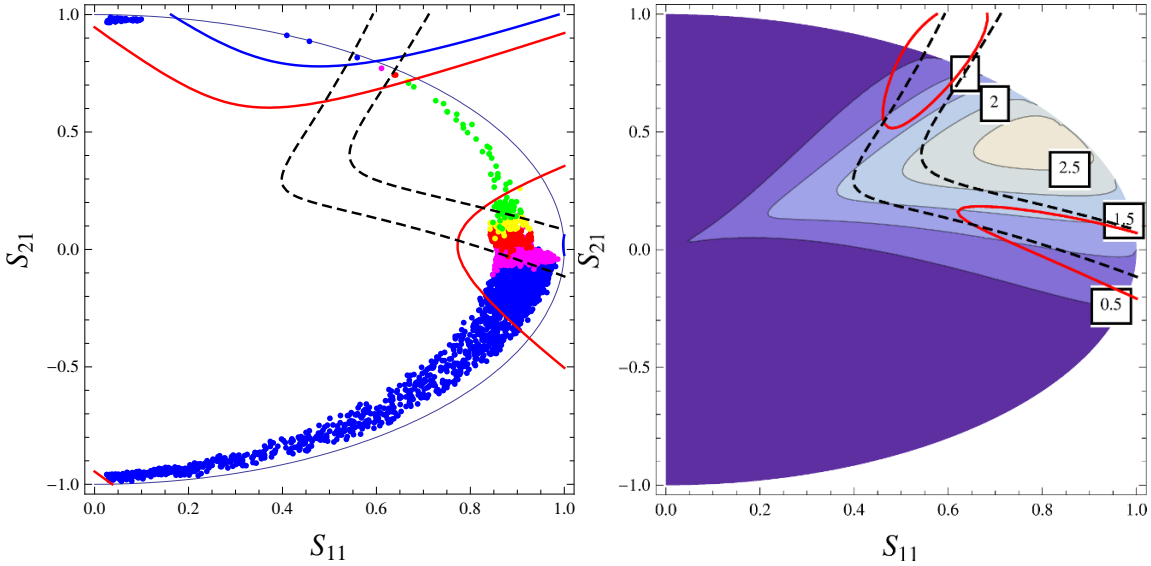

Figure 9. Left: subset of results of the "dynamical μ" scan shown in figure 8 plotted in terms of the mixing matrix parameters S_{11} and S_{21} where all point pass experimental limits (except Higgs branching ratios). The point colours denote the $\mu_{\gamma\gamma}$ values, varying from dark blue for $\mu_{\gamma\gamma} < 1$ to red with $1.33 < \mu_{\gamma\gamma} < 1.67$ to green for $\mu_{\gamma\gamma} > 2$. The solid contour lines show $\mu_{bb} = 0.6, 1.0$ (thick red, thick blue respectively) and $S_{11}^2 + S_{21}^2 = 1$ (thin blue) while the dashed black contours show $\mu_{WW} = 1.0 \pm 0.3$. Right: shown for comparison, this is a plot of the same form as figure 4 but with $\tan\beta = 1.5, \lambda v/m_f = -2$.

8 Conclusions

Dirac gaugino models are gaining increased interest as non-minimal supersymmetric standard models with enhanced naturalness compared to the MSSM and an enhanced Higgs mass that can also relax bounds on direct superpartner searches. With the latest update to the `SARAH` package, it is now possible to study such models quantitatively using modern numerical tools, and this work is a first step in exploring phenomenologically the low-energy parameter space. We have discussed the properties of three different Dirac gaugino scenarios that are subclasses of the minimal Dirac gaugino extension of the (N)MSSM: the "MSSM in disguise," the "MSSM without μ term" of [7] and a new scenario involving a dynamical μ term. While the first of these is phenomenologically very similar to the MSSM with higher-dimensional operators, we found that the second is unfortunately severely challenged by the current data. The third scenario, on the other hand, can be particularly natural and also has many characteristics appropriate to allow Higgs mixing and thus modifications of the Higgs production and decay rates; in particular, it is possible for example to enhance the diphoton signal, suppress the bottom and tau signals, while leaving the Z and W channels roughly the same as the Standard Model. We have performed a first examination of its parameter space but clearly it would be interesting to examine it further, particularly as new Higgs data becomes available.

There are now many interesting directions for future work. One will be to compare specific models directly with collider data, particularly in the context of models with light

JHEP06(2013)073

stops. In addition, it would be interesting to see how embedding the models we have discussed in particular high-energy completions affects the discussion of naturalness. Furthermore, constraints due to dark matter (assuming a thermal history of the universe or otherwise) can now also be applied. On the technical side, to further refine the precision of the Higgs mass, the leading two-loop corrections involving the Dirac gluinos should now be calculated. This work is therefore one step on the increasingly attractive path of bringing the phenomenology of Dirac gauginos closer to the level of understanding of the (N)MSSM.

Acknowledgments

We thank Jong Soo Kim, Nicolas Bernal and Werner Porod for fruitful discussions. MDG was supported by ERC advanced grant 226371. He would like to additionally thank Veronica Sanz and Michael Trott for helpful discussions, and Chris Wymant for pointing out some typos. KB is supported in part by the European contract "UNILHC" PITN-GA-2009-237920.

A Tree-level parameters of the model

In this section we summarise the tree-level parameters of the model; see also [23]. Here we add the tadpole term for the singlet and expressions for the stop and stau mass matrices including the new Dirac gaugino D-term corrections.

A.1 Higgs potential

It will be useful to introduce the following effective mass parameters:

$$\begin{aligned}\tilde{\mu} &= \mu + \frac{1}{\sqrt{2}}(\lambda_S\, v_S + \lambda_T\, v_T) \\ \tilde{B}\mu &= B\mu + \frac{\lambda_S}{\sqrt{2}}(M_S + A_S)v_S + \frac{\lambda_T}{\sqrt{2}}(M_T + A_T)v_T + \frac{1}{2}\lambda_S\,\kappa\, v_S^2\end{aligned} \tag{A.1}$$

A.1.1 Equations of motion for the CP-even neutral fields

The scalar potential for the CP-even neutral fields is given by:

$$\begin{aligned}V_{EW} = &\left[\frac{g^2+g'^2}{4}c_{2\beta}^2 \;+\; \frac{\lambda_S^2+\lambda_T^2}{2}s_{2\beta}^2\right]\frac{v^4}{8} \\ &+\left[m_{H_u}^2 s_\beta^2 + m_{H_d}^2 c_\beta^2 \;+\tilde{\mu}^2 - \tilde{B}\mu\, s_{2\beta} \;+(g\, m_{2D}\, v_T - g' m_{1D}\, v_S)c_{2\beta}\right]\frac{v^2}{2} \\ &+\sqrt{2}t_S v_S + \frac{\kappa^2}{4}v_S^4 + \frac{\kappa}{\sqrt{2}}\frac{(3M_S + A_\kappa)}{3}\,v_S^3 + \frac{1}{2}\tilde{m}_{SR}^2\, v_S^2 + \;\frac{1}{2}\tilde{m}_{TR}^2\, v_T^2\end{aligned} \tag{A.2}$$

where the effective masses for the real parts of the S and T fields read:

$$\tilde{m}_{SR}^2 = M_S^2 + m_S^2 + 4m_{1D}^2 + B_S, \qquad \tilde{m}_{TR}^2 = M_T^2 + m_T^2 + 4m_{2D}^2 + B_T \tag{A.3}$$

There is no restriction on the sign of the different mass parameters m_S^2 and B_S at this stage.

The imaginary parts of the fields have been dropped as their vevs are vanishing due to the assumed CP conservation [15]. The coefficients of the corresponding quadratic terms:

$$\tilde{m}_{SI}^2 = M_S^2 + m_S^2 - B_S, \qquad \tilde{m}_{TI}^2 = M_T^2 + m_T^2 - B_T \tag{A.4}$$

do not, in contrast to the CP-even partners, receive contributions from D-terms proportional to the Dirac masses.

As is customarily done for the (N)MSSM, the minimization of the scalar potential allows here also to express $\tilde{\mu}$ and $\tilde{B}\mu$ as a function of the other parameters:

$$\tilde{\mu}^2 + \frac{M_Z^2}{2} = \frac{m_{H_d}^2 - t_\beta^2\, m_{H_u}^2}{t_\beta^2 - 1} + \left[\frac{t_\beta^2 + 1}{t_\beta^2 - 1}\right]\left(g\, m_{2D}\, v_T - g' m_{1D}\, v_S\right) \tag{A.5}$$

and

$$M_A^2 \equiv \frac{2\tilde{B}\mu}{s_{2\beta}} = 2\tilde{\mu}^2 + m_{H_u}^2 + m_{H_d}^2 - \frac{\lambda_S^2 + \lambda_T^2}{2} v^2 c_\beta^2 \tag{A.6}$$

The new equations are

$$\begin{aligned} 0 &= \kappa^2 v_S^3 + \frac{\kappa}{\sqrt{2}}(A_\kappa + 3M_S) v_S^2 + \left(\tilde{m}_{SR}^2 + \lambda_S(\lambda_S - \kappa s_{2\beta})\frac{v^2}{2}\right) v_S + \sqrt{2} t_S + v_0^3 \\ 0 &= (2\tilde{m}_{TR}^2 + \lambda_T^2 v^2) v_T + v^2\left[g m_{2D} c_{2\beta} + \sqrt{2}\tilde{\mu}\lambda_T - \frac{\lambda_T}{\sqrt{2}}(M_T + A_T) s_{2\beta}\right] \end{aligned} \tag{A.7}$$

where

$$v_0^3 = -\frac{v^2}{2}\left[g' m_{1D} c_{2\beta} - \lambda_S\left(\sqrt{2}\mu - \frac{(A_S + M_S)}{\sqrt{2}} s_{2\beta} + \lambda_T v_T\right)\right]. \tag{A.8}$$

We can use these to solve for the masses in terms of the vevs. However, since the vev of T contributes to the W boson mass, the electroweak precision data give important bounds on the parameters of the model. For instance, using $\Delta\rho = (4.2 \pm 2.7) \times 10^{-4}$ [80–84], we require:

$$\Delta\rho \simeq 4\frac{v_T^2}{v^2} < 1 \times 10^{-3}\ (95\%) \tag{A.9}$$

which is satisfied for $v_T \lesssim 4\,\text{GeV}$. For large triplet masses we have

$$v_T \simeq \frac{v^2}{2\tilde{m}_{TR}^2}\left[-g m_{2D} c_{2\beta} - \sqrt{2}\tilde{\mu}\lambda_T + \frac{\lambda_T}{\sqrt{2}}(M_T + A_T) s_{2\beta}\right] \tag{A.10}$$

A.1.2 Masses of the CP even neutral scalars

Introducting the notation

$$\begin{aligned} \tilde{m}_S^2 &= \tilde{m}_{SR}^2 + \lambda_S^2\frac{v^2}{2} - \kappa\,\lambda_S\frac{v^2}{2} s_{2\beta} + 3\kappa^2 v_S^2 + \frac{\sqrt{2}}{3}\kappa\, v_S\,(A_\kappa + 3M_S) \\ \tilde{m}_T^2 &= \tilde{m}_{TR}^2 + \lambda_T^2\frac{v^2}{2} \end{aligned} \tag{A.11}$$

JHEP06(2013)073

the mass matrix for the CP even scalars in the basis $\{h, H, S_R, T_R^0\}$ is:

$$\begin{pmatrix} M_Z^2 + \Delta_h s_{2\beta}^2 & \Delta_h s_{2\beta} c_{2\beta} & \Delta_{hs} & \Delta_{ht} \\ \Delta_h s_{2\beta} c_{2\beta} & M_A^2 - \Delta_h s_{2\beta}^2 & \Delta_{Hs} & \Delta_{Ht} \\ \Delta_{hs} & \Delta_{Hs} & \tilde{m}_S^2 & \lambda_S \lambda_T \frac{v^2}{2} \\ \Delta_{ht} & \Delta_{Ht} & \lambda_S \lambda_T \frac{v^2}{2} & \tilde{m}_T^2 \end{pmatrix} \tag{A.12}$$

where we have defined:

$$\Delta_h = \frac{v^2}{2}(\lambda_S^2 + \lambda_T^2) - M_Z^2 \tag{A.13}$$

which vanishes when λ_S and λ_T take their $N = 2$ values [10]. We denote non-diagonal elements describing the mixing of S_R and T_R^0 states with the light Higgs h:

$$\Delta_{hs} = -2\frac{v_S}{v}\tilde{m}_{SR}^2 - \sqrt{2}\kappa\frac{v_S^2}{v}(A_\kappa + 3M_S) - 2\kappa^2\frac{v_S^3}{v}, \qquad \Delta_{ht} = -2\frac{v_T}{v}\tilde{m}_{TR}^2 \tag{A.14}$$

while

$$\Delta_{Hs} = g' m_{1D} v s_{2\beta} - \lambda_S \frac{v(A_s + M_s)}{\sqrt{2}} c_{2\beta}, \qquad \Delta_{Ht} = -g m_{2D} v s_{2\beta} - \lambda_T \frac{v(A_T + M_T)}{\sqrt{2}} c_{2\beta} \tag{A.15}$$

stand for the corresponding mixing with heavier Higgs, H.

Let us work with $M_S = M_T = A_S = A_\kappa = A_T = 0$. Rewriting the v_S equation we have

$$\begin{aligned} 0 &= \kappa^2 v_S^3 + \frac{\kappa}{\sqrt{2}}(A_\kappa + 3M_S)v_S^2 + \tilde{m}_{SR}^2 v_S + \sqrt{2}t_S \\ &\quad - \frac{v^2}{2}\left[g' m_{1D} c_{2\beta} - \lambda_S\left(\sqrt{2}\tilde{\mu} - \kappa s_{2\beta} v_S - \frac{(A_S + M_S)}{\sqrt{2}} s_{2\beta}\right)\right] \\ &\to \kappa^2 v_S^3 + \tilde{m}_{SR}^2 v_S + \sqrt{2}t_S - \frac{v^2}{2}\left[g' m_{1D} c_{2\beta} - \lambda_S\left(\sqrt{2}\tilde{\mu} - \kappa s_{2\beta} v_S\right)\right] = 0 \end{aligned} \tag{A.16}$$

Then using the minimisation conditions we can write

$$\begin{aligned} \Delta_{hs} &= v[v_S \lambda_S(\lambda_S - \kappa s_{2\beta}) - g' m_{1D} c_{2\beta} + \sqrt{2}\lambda_S \mu + \lambda_S \lambda_T v_T] \\ &= v[\sqrt{2}\lambda_S \tilde{\mu} - g' m_{1D} c_{2\beta} - \lambda_S v_S \kappa s_{2\beta}] \end{aligned} \tag{A.17}$$

Clearly $\Delta_{hs} \lesssim M_Z^2$ is necessary to prevent a see-saw reduction in the lightest Higgs mass. We have

$$\begin{aligned} \tilde{m}_{SR}^2 &= -\frac{1}{v_S}\left[\sqrt{2}t_S + \kappa^2 v_S^3 - \frac{v^2}{2} g' m_{1D} c_{2\beta} + \frac{v^2}{2}\lambda_S\left(\sqrt{2}\tilde{\mu} - \kappa s_{2\beta} v_S\right)\right] \\ &= -\frac{1}{v_S}\left[\sqrt{2}t_S + \kappa^2 v_S^3 + \frac{v}{2}\Delta_{hs}\right] \end{aligned} \tag{A.18}$$

A.2 Squark masses

The squark masses are modified by the Dirac mass terms via the D-term contribution. We give here the expressions for the mass matrices for stops, sbottoms and staus:

$$\begin{aligned} (\mathcal{M}_{\tilde{t}}^2)_{11} &= m_Q^2 + m_t^2 + \frac{1}{3} g_Y m_{D1} v_S + g_2 m_{D2} v_T + M_Z^2\left(\frac{1}{2} - \frac{2}{3}s_W^2\right) c_{2\beta} \\ (\mathcal{M}_{\tilde{t}}^2)_{21} &= m_t(A_t - \tilde{\mu}\cot\beta) \end{aligned}$$

$$(\mathcal{M}^2_{\tilde{t}})_{22} = m^2_{t_R} + m^2_t - \frac{4}{3} g_Y m_{D1} v_S + \frac{2}{3} M_Z^2 s_W^2 c_{2\beta} \tag{A.19}$$

The entries of the sbottom mass matrix read

$$\begin{aligned}
(\mathcal{M}^2_{\tilde{b}})_{11} &= m^2_Q + m^2_b + \frac{1}{3} g_Y m_{D1} v_S - g_2 m_{D2} v_T + M_Z^2 \Big(-\frac{1}{2} + \frac{1}{3} s_W^2 \Big) c_{2\beta} \\
(\mathcal{M}^2_{\tilde{b}})_{21} &= m_b (A_b - \tilde{\mu} \tan\beta) \\
(\mathcal{M}^2_{\tilde{b}})_{22} &= m^2_D + m^2_b + \frac{2}{3} g_Y m_{D1} v_S - \frac{1}{3} M_Z^2 s_W^2 c_{2\beta}
\end{aligned} \tag{A.20}$$

The entries of the stau mass matrix read

$$\begin{aligned}
(\mathcal{M}^2_{\tilde{\tau}})_{11} &= m^2_L + m^2_\tau - g_Y m_{D1} v_S - g_2 m_{D2} v_T + M_Z^2 \Big(-\frac{1}{2} + s_W^2 \Big) c_{2\beta} \\
(\mathcal{M}^2_{\tilde{\tau}})_{21} &= m_\tau (A_\tau - \tilde{\mu} \tan\beta) \\
(\mathcal{M}^2_{\tilde{\tau}})_{22} &= m^2_{\tau_R} + m^2_\tau + 2 g_Y m_{D1} v_S - M_Z^2 s_W^2 c_{2\beta}
\end{aligned} \tag{A.21}$$

B One-loop effective potential

The standard general form of the Higgs potential up to quartic order is

$$\begin{aligned}
V_{\text{eff}} \;=\; & (m^2_{H_u} + \mu^2)|H_u|^2 + (m^2_{H_d} + \mu^2)|H_d|^2 - [m^2_{12} H_u \cdot H_d + h.c.] \\
& + \frac{1}{2}\left[\frac{1}{4}(g^2 + g'^2) + \lambda_1\right](|H_d|^2)^2 + \frac{1}{2}\left[\frac{1}{4}(g^2 + g'^2) + \lambda_2\right](|H_u|^2)^2 \\
& + \left[\frac{1}{4}(g^2 - g'^2) + \lambda_3\right]|H_d|^2 |H_u|^2 + \left[-\frac{1}{2} g^2 + \lambda_4\right](H_d \cdot H_u)(H_d^* \cdot H_u^*) \\
& + \left(\frac{\lambda_5}{2}(H_d \cdot H_u)^2 + \left[\lambda_6 |H_d|^2 + \lambda_7 |H_u|^2\right](H_d \cdot H_u) + h.c.\right),
\end{aligned} \tag{B.1}$$

In Dirac gaugino models where we integrate out the heavy singlet and triplet scalars, we find λ_3 and λ_4 have a tree level contribution, so we write $\lambda_3 = 2\lambda_T^2 + \lambda_3'$, $\lambda_4 = \lambda_S^2 - \lambda_T^2 + \lambda_4'$ where λ_3', λ_4' are the loop corrections to the potential. Then we find at one loop $\lambda_4' = \lambda_5 = \lambda_6 = \lambda_7 = 0$, with the remaining contributions from the singlet and triplet scalars given by

$$\begin{aligned}
128\pi^2 \lambda_1 = \; & 4\lambda_S^4 \log\left[\tilde{m}^2_{SI} v^{-2}\right] + 4\lambda_S^4 \log\left[\tilde{m}^2_{SR} v^{-2}\right] + 4\lambda_T^4 \log\left[\tilde{m}^2_{TI} v^{-2}\right] + 4\lambda_T^4 \log\left[\tilde{m}^2_{TR} v^{-2}\right] \\
& + 8\Big(-\tilde{m}^2_{TI} + \tilde{m}^2_{SI}\Big)^{-1}\Big(-\tilde{m}^2_{TR} + \tilde{m}^2_{SR}\Big)^{-1} \lambda_S^2 \lambda_T^2 \Big(-2\tilde{m}^2_{SI}\tilde{m}^2_{SR} + 2\tilde{m}^2_{SR}\tilde{m}^2_{TI} + \\
& + 2\tilde{m}^2_{SI}\tilde{m}^2_{TR} - 2\tilde{m}^2_{TI}\tilde{m}^2_{TR} + \tilde{m}^2_{SI}\Big(-\tilde{m}^2_{TR} + \tilde{m}^2_{SR}\Big)\log\left[\tilde{m}^2_{SI} v^{-2}\right] \\
& + \tilde{m}^2_{SR}\Big(-\tilde{m}^2_{TI} + \tilde{m}^2_{SI}\Big)\log\left[\tilde{m}^2_{SR} v^{-2}\right] - \tilde{m}^2_{SR}\tilde{m}^2_{TI}\log\left[\tilde{m}^2_{TI} v^{-2}\right] + \tilde{m}^2_{TI}\tilde{m}^2_{TR}\log\left[\tilde{m}^2_{TI} v^{-2}\right] \\
& - \tilde{m}^2_{SI}\tilde{m}^2_{TR}\log\left[\tilde{m}^2_{TR} v^{-2}\right] + \tilde{m}^2_{TI}\tilde{m}^2_{TR}\log\left[\tilde{m}^2_{TR} v^{-2}\right]\Big) \\
& + 4\Big(-\tilde{m}^2_{TR} + \tilde{m}^2_{TI}\Big)^{-1}\Big(-\Big(-\tilde{m}^2_{TR} + \tilde{m}^2_{TI}\Big)\Big(-2\lambda_T^2 + g_2^2\Big)^2 \\
& + \Big(2\Big(3\tilde{m}^2_{TI} - \tilde{m}^2_{TR}\Big)\lambda_T^4 - 4g_2^2\tilde{m}^2_{TI}\lambda_T^2 + g_2^4\tilde{m}^2_{TI}\Big)\log\left[\tilde{m}^2_{TI} v^{-2}\right] \\
& + \Big(2\Big(-3\tilde{m}^2_{TR} + \tilde{m}^2_{TI}\Big)\lambda_T^4 + 4g_2^2\tilde{m}^2_{TR}\lambda_T^2 - g_2^4\tilde{m}^2_{TR}\Big)\log\left[\tilde{m}^2_{TR} v^{-2}\right]\Big)
\end{aligned} \tag{B.2}$$

JHEP06(2013)073

$$
\begin{aligned}
128\pi^2\lambda_2 = {} & 4\lambda_S^4 \log\left[\tilde{m}_{SI}^2 v^{-2}\right] + 4\lambda_S^4 \log\left[\tilde{m}_{SR}^2 v^{-2}\right] + 4\lambda_T^4 \log\left[\tilde{m}_{TI}^2 v^{-2}\right] + 4\lambda_T^4 \log\left[\tilde{m}_{TR}^2 v^{-2}\right] \\
& + 8\Big(-\tilde{m}_{TI}^2+\tilde{m}_{SI}^2\Big)^{-1}\Big(-\tilde{m}_{TR}^2+\tilde{m}_{SR}^2\Big)^{-1}\lambda_S^2\lambda_T^2\Big(-2\tilde{m}_{SI}^2\tilde{m}_{SR}^2+2\tilde{m}_{SR}^2\tilde{m}_{TI}^2+2\tilde{m}_{SI}^2\tilde{m}_{TR}^2 \\
& - 2\tilde{m}_{TI}^2\tilde{m}_{TR}^2 + \tilde{m}_{SI}^2\Big(-\tilde{m}_{TR}^2+\tilde{m}_{SR}^2\Big)\log\left[\tilde{m}_{SI}^2 v^{-2}\right] \\
& + \tilde{m}_{SR}^2\Big(-\tilde{m}_{TI}^2+\tilde{m}_{SI}^2\Big)\log\left[\tilde{m}_{SR}^2 v^{-2}\right] - \tilde{m}_{SR}^2\tilde{m}_{TI}^2\log\left[\tilde{m}_{TI}^2 v^{-2}\right] + \tilde{m}_{TI}^2\tilde{m}_{TR}^2\log\left[\tilde{m}_{TI}^2 v^{-2}\right] \\
& - \tilde{m}_{SI}^2\tilde{m}_{TR}^2\log\left[\tilde{m}_{TR}^2 v^{-2}\right] + \tilde{m}_{TI}^2\tilde{m}_{TR}^2\log\left[\tilde{m}_{TR}^2 v^{-2}\right]\Big) \\
& + 4\Big(-\tilde{m}_{TR}^2+\tilde{m}_{TI}^2\Big)^{-1}\Big(-\Big(-\tilde{m}_{TR}^2+\tilde{m}_{TI}^2\Big)\Big(-2\lambda_T^2+g_2^2\Big)^2 \\
& + \Big(2\Big(3\tilde{m}_{TI}^2-\tilde{m}_{TR}^2\Big)\lambda_T^4 - 4g_2^2\tilde{m}_{TI}^2\lambda_T^2 + g_2^4\tilde{m}_{TI}^2\Big)\log\left[\tilde{m}_{TI}^2 v^{-2}\right] \\
& + \Big(2\Big(-3\tilde{m}_{TR}^2+\tilde{m}_{TI}^2\Big)\lambda_T^4 + 4g_2^2\tilde{m}_{TR}^2\lambda_T^2 - g_2^4\tilde{m}_{TR}^2\Big)\log\left[\tilde{m}_{TR}^2 v^{-2}\right]\Big) \qquad \text{(B.3)} \\
64\pi^2\lambda_3' = {} & 2\lambda_S^4 \log\left[\tilde{m}_{SI}^2 v^{-2}\right] + 2\lambda_S^4 \log\left[\tilde{m}_{SR}^2 v^{-2}\right] + 2\lambda_T^4 \log\left[\tilde{m}_{TI}^2 v^{-2}\right] + 2\lambda_T^4 \log\left[\tilde{m}_{TR}^2 v^{-2}\right] \\
& - 4\Big(-\tilde{m}_{TI}^2+\tilde{m}_{SI}^2\Big)^{-1}\Big(-\tilde{m}_{TR}^2+\tilde{m}_{SR}^2\Big)^{-1}\lambda_S^2\lambda_T^2\Big(-2\tilde{m}_{SI}^2\tilde{m}_{SR}^2+2\tilde{m}_{SR}^2\tilde{m}_{TI}^2 \\
& + 2\tilde{m}_{SI}^2\tilde{m}_{TR}^2 - 2\tilde{m}_{TI}^2\tilde{m}_{TR}^2 + \tilde{m}_{SI}^2\Big(-\tilde{m}_{TR}^2+\tilde{m}_{SR}^2\Big)\log\left[\tilde{m}_{SI}^2 v^{-2}\right] \\
& + \tilde{m}_{SR}^2\Big(-\tilde{m}_{TI}^2+\tilde{m}_{SI}^2\Big)\log\left[\tilde{m}_{SR}^2 v^{-2}\right] - \tilde{m}_{SR}^2\tilde{m}_{TI}^2\log\left[\tilde{m}_{TI}^2 v^{-2}\right] + \tilde{m}_{TI}^2\tilde{m}_{TR}^2\log\left[\tilde{m}_{TI}^2 v^{-2}\right] \\
& - \tilde{m}_{SI}^2\tilde{m}_{TR}^2\log\left[\tilde{m}_{TR}^2 v^{-2}\right] + \tilde{m}_{TI}^2\tilde{m}_{TR}^2\log\left[\tilde{m}_{TR}^2 v^{-2}\right]\Big) \\
& + 2\Big(-\tilde{m}_{TR}^2+\tilde{m}_{TI}^2\Big)^{-1}\Big(-\Big(-\tilde{m}_{TR}^2+\tilde{m}_{TI}^2\Big)\Big(-2\lambda_T^2+g_2^2\Big)^2 \\
& + \Big(2\Big(3\tilde{m}_{TI}^2-\tilde{m}_{TR}^2\Big)\lambda_T^4 - 4g_2^2\tilde{m}_{TI}^2\lambda_T^2 + g_2^4\tilde{m}_{TI}^2\Big)\log\left[\tilde{m}_{TI}^2 v^{-2}\right] \\
& + \Big(2\Big(-3\tilde{m}_{TR}^2+\tilde{m}_{TI}^2\Big)\lambda_T^4 + 4g_2^2\tilde{m}_{TR}^2\lambda_T^2 - g_2^4\tilde{m}_{TR}^2\Big)\log\left[\tilde{m}_{TR}^2 v^{-2}\right]\Big) \qquad \text{(B.4)}
\end{aligned}
$$

Note that there are also important contributions from the stops and sbottoms, which at this level are identical to those in the MSSM (hence we separated them in equation (3.1)) except with the soft masses shifted by the Dirac gaugino D-term contributions as in equations (A.19) and (A.20).

C Experimental data

In this appendix we give the experimental data, current at time of writing, used in the text for crude 95% confidence level limits. The Higgs mass reported by CMS [85] and ATLAS [86] is

$$
m_H = 125.7\pm0.3(\text{stat})\pm0.3\text{sys GeV (CMS)}, 125.5\pm0.2(\text{stat})^{+0.5}_{-0.6}\text{sys GeV (ATLAS)}. \qquad \text{(C.1)}
$$

At the time of writing the first draft of this paper, both the CMS and ATLAS experiments were reporting excesses in the Higgs to $\gamma\gamma$ channel. In table 1 we give the values of μ_{ii} reported at that time (given in [1, 2, 87]). However, since then the rates have been revised, so that while ATLAS still reports an excess with a 2σ significance, CMS now finds a slight deficit. The latest values (announced at the Moriond conference), taken from [85, 86, 88], are given in table table 2.

JHEP06(2013)073

	CMS	ATLAS	Tevatron
$\mu_{\gamma\gamma}$	1.6 ± 0.4	1.8 ± 0.5	$3.62^{+2.96}_{-2.54}$
μ_{ZZ}	0.64 ± 0.57(7 TeV)	1.7 ± 1.1(7 TeV)	
	0.79 ± 0.56(8 TeV)	1.3 ± 0.8 (8 TeV)	
	$0.8^{+0.35}_{-0.28}$(combined, HCP)	1.4 ± 0.6 (combined, HCP)	
μ_{WW}	0.38 ± 0.56 (7 TeV)	0.5 ± 0.6 (7 TeV)	$0.32^{+1.13}_{-0.32}$
	0.98 ± 0.71 (8 TeV)	1.9 ± 0.7 (8 TeV)	
	0.74 ± 0.25(combined, HCP)	1.5 ± 0.6 (combined, HCP)	
μ_{bb}	0.59 ± 1.17 (7 TeV	0.46 ± 2.18 (7 TeV)	$1.97^{+0.74}_{-0.68}$
	0.41 ± 0.94 (8 TeV)		
	$1.3^{+0.7}_{-0.6}$(combined, HCP)	$-0.4 \pm 0.4 \pm 0.4$ (combined, HCP)	$1.56^{+0.72}_{-0.73}$(HCP)
$\mu_{\tau\tau}$	0.62 ± 1.17 (7 TeV)	0.45 ± 1.8 (7 TeV)	
	-0.72 ± 0.97 (8 TeV)		
	0.72 ± 0.52(combined, HCP)	0.7 ± 0.7 (combined, HCP)	

Table 1. Table of previous production cross-section times branching ratios over standard model values for CMS [2], ATLAS [1] and the Tevatron [89] including values reported at the HCP conference 2012 [87].

	CMS	ATLAS	Tevatron	Crude Average
$\mu_{\gamma\gamma}$	0.77 ± 0.27	1.6 ± 0.3	$3.62^{+2.96}_{-2.54}$	
μ_{ZZ}	0.92 ± 0.28	1.5 ± 0.4		1.11 ± 0.23
μ_{WW}	0.68 ± 0.2	1.0 ± 0.3	$0.32^{+1.13}_{-0.32}$	0.77 ± 0.16
μ_{bb}	1.15 ± 0.62	-0.4 ± 1.0	$1.97^{+0.74}_{-0.68}$	1.14 ± 0.43
$\mu_{\tau\tau}$	1.1 ± 0.41)	0.8 ± 0.7		1.02 ± 0.35

Table 2. Table of latest production cross-section times branching ratios over standard model values for CMS [85], ATLAS [86] (both using nearly 20 fb^{-1}) and the combined Tevatron search [88].

The limit for $\Delta\rho$ reported in [81–84] is

$$\Delta\rho = (4.2 \pm 2.7) \times 10^{-4}. \tag{C.2}$$

To get bounds from $b \to s\gamma$, we define the ratio of SUSY to SM contributions [90–95]

$$R \equiv \frac{\mathrm{BR}(b \to s\gamma)_{\mathrm{SUSY}}}{\mathrm{BR}(b \to s\gamma)_{\mathrm{SM}}} \tag{C.3}$$

Adding to the uncertainty of the SM prediction $\mathrm{Br}(B \to X_s\gamma)_{\mathrm{SM}} = (3.15 \pm 0.23) \cdot 10^{-4}$ an intrinsic SUSY error of 0.15 as well as the error of the experimental world average $\mathrm{Br}(B \to X_s\gamma)_{\mathrm{exp}} = (3.43 \pm 0.22) \cdot 10^{-4}$ [96], leads to the following 95% CL bound

$$R = [0.87, 1.31]\,. \tag{C.4}$$

JHEP06(2013)073

To generate the crude 95% confidence level limits in the text, we simply take the observables from table 2, combine with the above values for ρ and $\mathrm{Br}(B \to X_s\gamma)$, compute the value for χ^2, and compare to the 95% limit from the χ^2 distribution with the corresponding number of variables. Since we are doing a crude analysis, where there are duplicate values for the same observable we simply take the weighted mean and add the errors in inverse quadrature (i.e. $\frac{1}{\sigma^2} = \frac{1}{\sigma_1^2} + \frac{1}{\sigma_2^2}$), *with one exception*: since this paper is partly concerned with methods of obtaining excesses from the Higgs diphoton rate, we exclude that data from the fit, since the combined CMS and ATLAS value now barely shows an excess. Since the two values differ substantially compared to their errors, we take the opinion that it is not reasonable to combine them and that the CMS value may in principle be revised again.

References

[1] ATLAS collaboration, *Observation of a new particle in the search for the Standard Model Higgs boson with the ATLAS detector at the LHC*, *Phys. Lett.* **B 716** (2012) 1 [arXiv:1207.7214] [INSPIRE].

[2] CMS collaboration, *Observation of a new boson at a mass of* 125 *GeV with the CMS experiment at the LHC*, *Phys. Lett.* **B 716** (2012) 30 [arXiv:1207.7235] [INSPIRE].

[3] P. Fayet, *Massive gluinos*, *Phys. Lett.* **B 78** (1978) 417 [INSPIRE].

[4] J. Polchinski and L. Susskind, *Breaking of supersymmetry at intermediate-energy*, *Phys. Rev.* **D 26** (1982) 3661 [INSPIRE].

[5] L. Hall and L. Randall, $\mathrm{U}(1)_R$ *symmetric supersymmetry*, *Nucl. Phys.* **B 352** (1991) 289 [INSPIRE].

[6] P.J. Fox, A.E. Nelson and N. Weiner, *Dirac gaugino masses and supersoft supersymmetry breaking*, *JHEP* **08** (2002) 035 [hep-ph/0206096] [INSPIRE].

[7] A.E. Nelson, N. Rius, V. Sanz and M. Ünsal, *The minimal supersymmetric model without a* μ *term*, *JHEP* **08** (2002) 039 [hep-ph/0206102] [INSPIRE].

[8] I. Antoniadis, A. Delgado, K. Benakli, M. Quirós and M. Tuckmantel, *Splitting extended supersymmetry*, *Phys. Lett.* **B 634** (2006) 302 [hep-ph/0507192] [INSPIRE].

[9] I. Antoniadis, K. Benakli, A. Delgado, M. Quirós and M. Tuckmantel, *Split extended supersymmetry from intersecting branes*, *Nucl. Phys.* **B 744** (2006) 156 [hep-th/0601003] [INSPIRE].

[10] I. Antoniadis, K. Benakli, A. Delgado and M. Quirós, *A new gauge mediation theory*, *Adv. Stud. Theor. Phys.* **2** (2008) 645 [hep-ph/0610265] [INSPIRE].

[11] K. Hsieh, *Pseudo-Dirac bino dark matter*, *Phys. Rev.* **D 77** (2008) 015004 [arXiv:0708.3970] [INSPIRE].

[12] S.D.L. Amigo, A.E. Blechman, P.J. Fox and E. Poppitz, *R-symmetric gauge mediation*, *JHEP* **01** (2009) 018 [arXiv:0809.1112] [INSPIRE].

JHEP06(2013)073

[13] A.E. Blechman, *R-symmetric gauge mediation and the minimal R-symmetric supersymmetric Standard Model*, *Mod. Phys. Lett.* **A 24** (2009) 633 [arXiv:0903.2822] [INSPIRE].

[14] K. Benakli and M. Goodsell, *Dirac gauginos in general gauge mediation*, *Nucl. Phys.* **B 816** (2009) 185 [arXiv:0811.4409] [INSPIRE].

[15] G. Bélanger, K. Benakli, M. Goodsell, C. Moura and A. Pukhov, *Dark matter with Dirac and Majorana gaugino masses*, *JCAP* **08** (2009) 027 [arXiv:0905.1043] [INSPIRE].

[16] K. Benakli and M. Goodsell, *Dirac gauginos and kinetic mixing*, *Nucl. Phys.* **B 830** (2010) 315 [arXiv:0909.0017] [INSPIRE].

[17] E.J. Chun, J.-C. Park and S. Scopel, *Dirac gaugino as leptophilic dark matter*, *JCAP* **02** (2010) 015 [arXiv:0911.5273] [INSPIRE].

[18] K. Benakli and M. Goodsell, *Dirac gauginos, gauge mediation and unification*, *Nucl. Phys.* **B 840** (2010) 1 [arXiv:1003.4957] [INSPIRE].

[19] L.M. Carpenter, *Dirac gauginos, negative supertraces and gauge mediation*, *JHEP* **09** (2012) 102 [arXiv:1007.0017] [INSPIRE].

[20] G.D. Kribs, T. Okui and T.S. Roy, *Viable gravity-mediated supersymmetry breaking*, *Phys. Rev.* **D 82** (2010) 115010 [arXiv:1008.1798] [INSPIRE].

[21] E.J. Chun, *Leptogenesis origin of Dirac gaugino dark matter*, *Phys. Rev.* **D 83** (2011) 053004 [arXiv:1009.0983] [INSPIRE].

[22] S. Choi, D. Choudhury, A. Freitas, J. Kalinowski and P. Zerwas, *The extended Higgs system in R-symmetric supersymmetry theories*, *Phys. Lett.* **B 697** (2011) 215 [*Erratum ibid.* **B 698** (2011) 457] [arXiv:1012.2688] [INSPIRE].

[23] K. Benakli, M.D. Goodsell and A.-K. Maier, *Generating μ and $B\mu$ in models with Dirac gauginos*, *Nucl. Phys.* **B 851** (2011) 445 [arXiv:1104.2695] [INSPIRE].

[24] S. Abel and M. Goodsell, *Easy Dirac gauginos*, *JHEP* **06** (2011) 064 [arXiv:1102.0014] [INSPIRE].

[25] P. Kumar and E. Ponton, *Electroweak baryogenesis and dark matter with an approximate R-symmetry*, *JHEP* **11** (2011) 037 [arXiv:1107.1719] [INSPIRE].

[26] K. Benakli, *Dirac gauginos: a user manual*, *Fortsch. Phys.* **59** (2011) 1079 [arXiv:1106.1649] [INSPIRE].

[27] R. Davies, J. March-Russell and M. McCullough, *A supersymmetric one Higgs doublet model*, *JHEP* **04** (2011) 108 [arXiv:1103.1647] [INSPIRE].

[28] R. Davies and M. McCullough, *Small neutrino masses due to R-symmetry breaking for a small cosmological constant*, *Phys. Rev.* **D 86** (2012) 025014 [arXiv:1111.2361] [INSPIRE].

[29] M. Heikinheimo, M. Kellerstein and V. Sanz, *How many supersymmetries?*, *JHEP* **04** (2012) 043 [arXiv:1111.4322] [INSPIRE].

[30] K. Rehermann and C.M. Wells, *Weak scale leptogenesis, R-symmetry and a displaced Higgs*, arXiv:1111.0008 [INSPIRE].

[31] G.D. Kribs and A. Martin, *Supersoft supersymmetry is super-safe*, *Phys. Rev.* **D 85** (2012) 115014 [arXiv:1203.4821] [INSPIRE].

[32] C. Frugiuele and T. Gregoire, *Making the sneutrino a Higgs with a $\mathrm{U}(1)_R$ lepton number*, *Phys. Rev.* **D 85** (2012) 015016 [arXiv:1107.4634] [INSPIRE].

JHEP06(2013)073

[33] E. Bertuzzo and C. Frugiuele, *Fitting neutrino physics with a $U(1)_R$ lepton number*, *JHEP* **05** (2012) 100 [arXiv:1203.5340] [INSPIRE].

[34] C. Frugiuele, T. Gregoire, P. Kumar and E. Ponton, *'$L = R$' — $U(1)_R$ as the origin of leptonic 'RPV'*, *JHEP* **03** (2013) 156 [arXiv:1210.0541] [INSPIRE].

[35] R. Davies, *Dirac gauginos and unification in F-theory*, *JHEP* **10** (2012) 010 [arXiv:1205.1942] [INSPIRE].

[36] R. Argurio, M. Bertolini, L. Di Pietro, F. Porri and D. Redigolo, *Holographic correlators for general gauge mediation*, *JHEP* **08** (2012) 086 [arXiv:1205.4709] [INSPIRE].

[37] I. Jack and D. Jones, *Nonstandard soft supersymmetry breaking*, *Phys. Lett.* **B 457** (1999) 101 [hep-ph/9903365] [INSPIRE].

[38] I. Jack and D. Jones, *Quasiinfrared fixed points and renormalization group invariant trajectories for nonholomorphic soft supersymmetry breaking*, *Phys. Rev.* **D 61** (2000) 095002 [hep-ph/9909570] [INSPIRE].

[39] M.D. Goodsell, *Two-loop RGEs with Dirac gaugino masses*, *JHEP* **01** (2013) 066 [arXiv:1206.6697] [INSPIRE].

[40] C. Brust, A. Katz, S. Lawrence and R. Sundrum, *SUSY, the third generation and the LHC*, *JHEP* **03** (2012) 103 [arXiv:1110.6670] [INSPIRE].

[41] M. Papucci, J.T. Ruderman and A. Weiler, *Natural SUSY endures*, *JHEP* **09** (2012) 035 [arXiv:1110.6926] [INSPIRE].

[42] J.R. Espinosa, C. Grojean, V. Sanz and M. Trott, *NSUSY fits*, *JHEP* **12** (2012) 077 [arXiv:1207.7355] [INSPIRE].

[43] G.D. Kribs, E. Poppitz and N. Weiner, *Flavor in supersymmetry with an extended R-symmetry*, *Phys. Rev.* **D 78** (2008) 055010 [arXiv:0712.2039] [INSPIRE].

[44] ATLAS collaboration, *Search for squarks and gluinos with the ATLAS detector using final states with jets and missing transverse momentum and* $5.8\,\text{fb}^{-1}$ *of* $\sqrt{s} = 8$ *TeV proton-proton collision data*, ATLAS-CONF-2012-109, CERN, Geneva Switzerland (2012).

[45] ATLAS collaboration, *Search for gluino pair production in final states with missing transverse momentum and at least three b-jets using* $12.8\,\text{fb}^{-1}$ *of pp collisions at* $\sqrt{s} = 8$ *TeV with the ATLAS Detector.*, ATLAS-CONF-2012-145, CERN, Geneva Switzerland (2012).

[46] ATLAS collaboration, *Search for direct production of the top squark in the all-hadronic* $t\bar{t} + E_T^{\text{miss}}$ *final state in* $21\,\text{fb}^{-1}$ *of pp collisions at* $\sqrt{s} = 8$ *TeV with the ATLAS detector*, ATLAS-CONF-2013-024, CERN, Geneva Switzerland (2013).

[47] ATLAS collaboration, *Search for direct production of charginos and neutralinos in events with three leptons and missing transverse momentum in* $21\,\text{fb}^{-1}$ *of pp collisions at* $\sqrt{s} = 8$ *TeV with the ATLAS detector*, ATLAS-CONF-2013-035, CERN, Geneva Switzerland (2013).

[48] F. Staub, SARAH , arXiv:0806.0538 [INSPIRE].

[49] F. Staub, *From superpotential to model files for FeynArts and CalcHep/CompHEP*, *Comput. Phys. Commun.* **181** (2010) 1077 [arXiv:0909.2863] [INSPIRE].

[50] F. Staub, *Automatic calculation of supersymmetric renormalization group equations and self energies*, *Comput. Phys. Commun.* **182** (2011) 808 [arXiv:1002.0840] [INSPIRE].

JHEP06(2013)073

[51] F. Staub, SARAH 3.2: *Dirac gauginos, UFO output and more*, *Comput. Phys. Commun.* **184** (2013) pp. 1792–1809 [arXiv:1207.0906] [INSPIRE].

[52] R.M. Fonseca, M. Malinsky, W. Porod and F. Staub, *Running soft parameters in SUSY models with multiple* U(1) *gauge factors*, *Nucl. Phys.* **B 854** (2012) 28 [arXiv:1107.2670] [INSPIRE].

[53] W. Porod, SPheno, *a program for calculating supersymmetric spectra, SUSY particle decays and SUSY particle production at* e^+e^- *colliders*, *Comput. Phys. Commun.* **153** (2003) 275 [hep-ph/0301101] [INSPIRE].

[54] W. Porod and F. Staub, SPheno 3.1: *extensions including flavour, CP-phases and models beyond the MSSM*, *Comput. Phys. Commun.* **183** (2012) 2458 [arXiv:1104.1573] [INSPIRE].

[55] H. Arason et al., *Renormalization group study of the Standard Model and its extensions. 1. The Standard Model*, *Phys. Rev.* **D 46** (1992) 3945 [INSPIRE].

[56] F. Staub, W. Porod and B. Herrmann, *The electroweak sector of the NMSSM at the one-loop level*, *JHEP* **10** (2010) 040 [arXiv:1007.4049] [INSPIRE].

[57] M. Spira, A. Djouadi, D. Graudenz and P. Zerwas, *Higgs boson production at the LHC*, *Nucl. Phys.* **B 453** (1995) 17 [hep-ph/9504378] [INSPIRE].

[58] A. Djouadi, M. Spira and P. Zerwas, *QCD corrections to hadronic Higgs decays*, *Z. Phys.* **C 70** (1996) 427 [hep-ph/9511344] [INSPIRE].

[59] H. Dreiner, K. Nickel, W. Porod and F. Staub, *Precise predictions for* $BR(B^0_{s,d} \to \ell\bar{\ell})$ *in models beyond the MSSM with* SARAH *and* SPheno , arXiv:1212.5074 [INSPIRE].

[60] A. Pukhov, *CalcHEP* 2.3: *MSSM, structure functions, event generation, batchs and generation of matrix elements for other packages*, hep-ph/0412191 [INSPIRE].

[61] E. Boos, M. Dubinin, V. Ilyin, A. Pukhov and V. Savrin, *CompHEP: specialized package for automatic calculations of elementary particle decays and collisions*, hep-ph/9503280 [INSPIRE].

[62] W. Kilian, T. Ohl and J. Reuter, *WHIZARD: simulating multi-particle processes at LHC and ILC*, *Eur. Phys. J.* **C 71** (2011) 1742 [arXiv:0708.4233] [INSPIRE].

[63] M. Moretti, T. Ohl and J. Reuter, *O'Mega: an optimizing matrix element generator*, hep-ph/0102195 [INSPIRE].

[64] T. Hahn, *Generating Feynman diagrams and amplitudes with FeynArts* 3, *Comput. Phys. Commun.* **140** (2001) 418 [hep-ph/0012260] [INSPIRE].

[65] T. Hahn, *FormCalc* 6, PoS(ACAT08)121 [arXiv:0901.1528] [INSPIRE].

[66] C. Degrande et al., *UFO — the Universal FeynRules Output*, *Comput. Phys. Commun.* **183** (2012) 1201 [arXiv:1108.2040] [INSPIRE].

[67] J. Alwall, M. Herquet, F. Maltoni, O. Mattelaer and T. Stelzer, *MadGraph* 5: *going beyond*, *JHEP* **06** (2011) 128 [arXiv:1106.0522] [INSPIRE].

[68] G. Bélanger, F. Boudjema, A. Pukhov and A. Semenov, *MicrOMEGAs* 2.0: *a program to calculate the relic density of dark matter in a generic model*, *Comput. Phys. Commun.* **176** (2007) 367 [hep-ph/0607059] [INSPIRE].

[69] H.E. Haber and R. Hempfling, *The renormalization group improved Higgs sector of the minimal supersymmetric model*, *Phys. Rev.* **D 48** (1993) 4280 [hep-ph/9307201] [INSPIRE].

JHEP06(2013)073

[70] A. Djouadi et al., *Supersymmetric contributions to electroweak precision observables: QCD corrections*, *Phys. Rev. Lett.* **78** (1997) 3626 [hep-ph/9612363] [INSPIRE].

[71] S. Heinemeyer, W. Hollik and G. Weiglein, *Electroweak precision observables in the minimal supersymmetric Standard Model*, *Phys. Rept.* **425** (2006) 265 [hep-ph/0412214] [INSPIRE].

[72] R. Barbieri, L.J. Hall, Y. Nomura and V.S. Rychkov, *Supersymmetry without a light Higgs boson*, *Phys. Rev.* **D 75** (2007) 035007 [hep-ph/0607332] [INSPIRE].

[73] L.J. Hall, D. Pinner and J.T. Ruderman, *A natural SUSY Higgs near* 126 *GeV*, *JHEP* **04** (2012) 131 [arXiv:1112.2703] [INSPIRE].

[74] CERN Yellow Pages, *SM Higgs branching ratios and partial-decay widths webpage*, http://twiki.cern.ch/twiki/bin/view/LHCPhysics/CERNYellowReportPageBR2.

[75] A. Delgado, G. Nardini and M. Quirós, *Large diphoton Higgs rates from supersymmetric triplets*, *Phys. Rev.* **D 86** (2012) 115010 [arXiv:1207.6596] [INSPIRE].

[76] K. Schmidt-Hoberg and F. Staub, *Enhanced $h \to \gamma\gamma$ rate in MSSM singlet extensions*, *JHEP* **10** (2012) 195 [arXiv:1208.1683] [INSPIRE].

[77] M. Carena, S. Gori, N.R. Shah, C.E. Wagner and L.-T. Wang, *Light stau phenomenology and the Higgs $\gamma\gamma$ rate*, *JHEP* **07** (2012) 175 [arXiv:1205.5842] [INSPIRE].

[78] R. Sato, K. Tobioka and N. Yokozaki, *Enhanced diphoton signal of the Higgs boson and the muon g-2 in gauge mediation models*, *Phys. Lett.* **B 716** (2012) 441 [arXiv:1208.2630] [INSPIRE].

[79] Particle Data Group collaboration, K. Nakamura et al., *Review of particle physics*, *J. Phys.* **G 37** (2010) 075021 [INSPIRE].

[80] Particle Data Group collaboration, C. Amsler et al., *Review of particle physics*, *Phys. Lett.* **B 667** (2008) 1 [INSPIRE].

[81] CDF collaboration, T. Aaltonen et al., *Precise measurement of the W-boson mass with the CDF II detector*, *Phys. Rev. Lett.* **108** (2012) 151803 [arXiv:1203.0275] [INSPIRE].

[82] D0 collaboration, V.M. Abazov et al., *Measurement of the W boson mass with the D0 detector*, *Phys. Rev. Lett.* **108** (2012) 151804 [arXiv:1203.0293] [INSPIRE].

[83] CDF, D0 and Tevatron Electroweak Working Group collaborations, T.E.W. Group, 2012 *update of the combination of CDF and D0 results for the mass of the W boson*, arXiv:1204.0042 [INSPIRE].

[84] V. Barger, P. Huang, M. Ishida and W.-Y. Keung, *Scalar-top masses from SUSY loops with* 125 *GeV* m_h *and precise* M_w, *Phys. Lett.* **B 718** (2013) 1024 [arXiv:1206.1777] [INSPIRE].

[85] CMS collaboration, *Combination of Standard Model Higgs boson searches and measurements of the properties of the new boson with a mass near* 125 *GeV*, CMS-PAS-HIG-13-005, CERN, Geneva Switzerland (2013).

[86] ATLAS collaboration, *Combined measurements of the mass and signal strength of the Higgs-like boson with the ATLAS detector using up to* 25 fb^{-1} *of proton-proton collision data*, ATLAS-CONF-2013-014, CERN, Geneva Switzerland (2013).

[87] *Hadron collider physics symposium* 2012 *webpage*, http://www.icepp.s.u-tokyo.ac.jp/hcp2012/.

JHEP06(2013)073

[88] Tevatron New Physics Higgs Working Group, CDF and D0 collaborations, *Updated combination of CDF and D0 searches for Standard Model Higgs boson production with up to* $10.0\,\text{fb}^{-1}$ *of data*, arXiv:1207.0449 [INSPIRE].

[89] Tevatron New Physics Higgs Working Group, CDF and D0 collaborations, *Updated combination of CDF and D0 searches for Standard Model Higgs boson production with up to* $10.0\,\text{fb}^{-1}$ *of data*, arXiv:1207.0449 [INSPIRE].

[90] M. Misiak and M. Steinhauser, *Three loop matching of the dipole operators for* $b \to s\gamma$ *and* $b \to sg$, *Nucl. Phys.* **B 683** (2004) 277 [hep-ph/0401041] [INSPIRE].

[91] M. Misiak and M. Steinhauser, *NNLO QCD corrections to the* $\bar{B} \to X_s\gamma$ *matrix elements using interpolation in* m_c, *Nucl. Phys.* **B 764** (2007) 62 [hep-ph/0609241] [INSPIRE].

[92] M. Misiak et al., *Estimate of* $B(\bar{B} \to X_s\gamma)$ *at* $O(\alpha_s^2)$, *Phys. Rev. Lett.* **98** (2007) 022002 [hep-ph/0609232] [INSPIRE].

[93] A. Freitas and U. Haisch, $\bar{B} \to X_s\gamma$ *in two universal extra dimensions*, *Phys. Rev.* **D 77** (2008) 093008 [arXiv:0801.4346] [INSPIRE].

[94] Heavy Flavor Averaging Group collaboration, D. Asner et al., *Averages of b-hadron, c-hadron and* τ*-lepton Properties*, arXiv:1010.1589 [INSPIRE].

[95] BaBar collaboration, J. Lees et al., *Measurement of* $B(B \to X_s\gamma)$*, the* $B \to X_s\gamma$ *photon energy spectrum and the direct CP asymmetry in* $B \to X_{s+d}\gamma$ *decays*, *Phys. Rev.* **D 86** (2012) 112008 [arXiv:1207.5772] [INSPIRE].

[96] Heavy Flavor Averaging Group collaboration, Y. Amhis et al., *Averages of b-hadron, c-hadron and* τ*-lepton properties as of early* 2012, arXiv:1207.1158 [INSPIRE].

JHEP06(2013)073